

---

## Polaritons in van der Waals heterostructures

Xiangdong Guo<sup>1,2#</sup>, Wei Lyu<sup>1,2#</sup>, Tinghan Chen<sup>1,3</sup>, Yang Luo<sup>1,3</sup>, Chenchen Wu<sup>1,2</sup>, Bei Yang<sup>1,2</sup>, Zhipei Sun<sup>4</sup>, F. Javier García de Abajo<sup>5,6</sup>, Xiaoxia Yang<sup>1,2\*</sup>, Qing Dai<sup>1,2\*</sup>

<sup>1</sup>CAS Key Laboratory of Nanophotonic Materials and Devices, CAS Key Laboratory of Standardization and Measurement for Nanotechnology, CAS Center for Excellence in Nanoscience, National Center for Nanoscience and Technology, Beijing 100190, China.

<sup>2</sup>Center of Materials Science and Optoelectronics Engineering, University of Chinese Academy of Sciences, Beijing 100049, China.

<sup>3</sup>School of Life Science, Peking University, Beijing 100871, China.

<sup>4</sup>Department of Electronics and Nanoengineering and QTF Centre of Excellence, Department of Applied Physics, Aalto University, Espoo 02150, Finland.

<sup>5</sup>ICFO-Institut de Ciències Fotoniques, The Barcelona Institute of Science and Technology, 08860 Castelldefels (Barcelona), Spain.

<sup>6</sup>ICREA-Institució Catalana de Recerca i Estudis Avançats, Passeig Lluís Companys 23, 08010 Barcelona, Spain.

\*emails: [daiq@nanoctr.cn](mailto:daiq@nanoctr.cn), [yangxx@nanoctr.cn](mailto:yangxx@nanoctr.cn)

**Abstract:** Two-dimensional (2D) monolayers supporting a wide variety of highly confined plasmons, phonon polaritons, and exciton polaritons can be vertically stacked in vdWHs with controlled constituent layers, stacking sequence, and even twist angles. Van der Waals heterostructures (vdWHs) combine advantages of 2D material polaritons, rich optical

This article has been accepted for publication and undergone full peer review but has not been through the copyediting, typesetting, pagination and proofreading process, which may lead to differences between this version and the [Version of Record](#). Please cite this article as [doi: 10.1002/adma.202201856](#).

This article is protected by copyright. All rights reserved.

structure design and atomic scale integration, which have greatly extended the performance and functions of polaritons, such as wide frequency range, long lifetime, ultrafast all-optical modulation, and photonic crystals for nanoscale light. Here, we review the state of the art of 2D material polaritons in vdWHs from the perspective of design principles and potential applications. We start by discussing some fundamental properties of polaritons in vdWHs, and then cover recent discoveries of plasmons, phonon polaritons, exciton polaritons and their hybrid modes in vdWHs, respectively. We conclude with a perspective discussion on potential applications of these polaritons such as nanophotonic integrated circuits, which will benefit from the intersection between nanophotonics and materials science.

## Contents

### 1. Introduction

### 2. Mechanisms of polariton modulation in vdWHs

### 3. Plasmons in vdWHs

#### 3.1 Band structure engineering

##### 3.1.1 Voltage-gated plasmonic devices with high quality

##### 3.1.2 Plasmon modulation through chemical and optical doping

##### 3.1.3 Modifying plasmons through moiré patterns

#### 3.2 Plasmon coupling to other quasi-particles

#### 3.3 Designing plasmons with optical structures and dielectrics

### 4. Phonon and exciton polaritons in vdWHs

#### 4.1 Tuning phonon polaritons in vdWHs

- 4.1.1 Dielectric engineering
- 4.1.2 Coupling via optical structures
- 4.1.3 Band structure and strain engineering
- 4.1.4 Coupling to molecular vibrations
- 4.2 Exciton polaritons in vdWHs
  - 4.2.1 Integration in optical structures
  - 4.2.2 Moiré exciton polaritons in twisted vdWHs
  - 4.2.3 Charge carrier manipulation
- 5. Polariton-polariton coupling in vdWHs**
  - 5.1 Plasmon-plasmon coupling
  - 5.2 Coupling between phonon polaritons
  - 5.3 Hybridization between plasmons and phonon polaritons
- 6. Perspectives**
  - 6.1 Light/polariton sources
  - 6.2 Optical waveguides
  - 6.3 Optical modulators and logic gates
  - 6.4 Detectors

## 1. Introduction

Tunable nanophotonic systems that can be integrated with silicon and manipulate light at deep-subwavelength scales is of paramount importance for photonic integrated circuits<sup>[1]</sup>, enhanced light-matter interaction<sup>[2]</sup>, sub-diffraction imaging<sup>[3]</sup>, metamaterials<sup>[4]</sup>, and negative refraction<sup>[5]</sup> among other feats. In particular, polaritons in two-dimensional (2D) materials exhibit the highest degree of mode confinement<sup>[6]</sup>. A variety of highly confined polaritons with unique properties<sup>[6-7]</sup> have been demonstrated in 2D materials, e.g. electrically tunable plasmons in graphene<sup>[7a, 8]</sup>, ultra-low-loss phonon polaritons in h-BN<sup>[9]</sup> and  $\alpha$ -MoO<sub>3</sub><sup>[7c, 7d]</sup>, room-temperature exciton polaritons in MoSe<sub>2</sub><sup>[10]</sup>, WSe<sub>2</sub><sup>[11]</sup> and CsPbBr<sub>3</sub> microsheets<sup>[12]</sup>, and Cooper-pair polaritons<sup>[13]</sup>. These polaritons have prompted the exploration of multiple potential applications, such as surface-enhanced infrared spectroscopy<sup>[8a, 14]</sup>, optical sensors<sup>[15]</sup>, nanolasers<sup>[16]</sup>, light modulators<sup>[17]</sup>, and nanophotonic circuits<sup>[18]</sup>. However, in most practical applications, important challenges, such as relatively large optical loss, reduced operation frequency range, and slow modulation speed, are remaining.

The hybrid light-matter nature of polaritons (i.e., quasiparticles made up of a photon strongly coupled to an electric dipole) can be passively tuned by designing the composition and geometry of the hosting materials<sup>[9, 19]</sup>, offering important advantages for nanophotonic systems<sup>[6a, 20]</sup>. Recently, van der Waals (vdW) heterostructures (vdWHs), which can be fabricated by exfoliating 2D materials down to isolated monolayers and subsequently reassembling them in a layer by layer fashion in precisely chosen compositions, stacking sequence, and twist angles, provide a versatile way to customize polaritons<sup>[21]</sup>. For example, the ultralong lifetime graphene plasmons in graphene/h-BN vdWHs<sup>[7a, 22]</sup>, efficient all-optical modulation of graphene plasmons in the graphene/monolayer MoS<sub>2</sub> vdWHs<sup>[23]</sup>, strong plasmonic nonlinear response in graphene/metal heterostructures<sup>[24]</sup> have been demonstrated. Moreover, the behavior of polaritons can also be modulated by creating moiré patterns in the vdWHs, for example, the extremely long plasmon lifetimes ( $\sim$ 3 ps) in stacked bilayer

graphene<sup>[25]</sup>, the photonic crystals of twisted bilayer graphene<sup>[26]</sup>, and tunable topological transitions of phonon polaritons in twisted  $\alpha$ -MoO<sub>3</sub> bilayers<sup>[27]</sup>.

Rapid progress in vdWHs fabrication is quickly opening a vast space for the design of polariton-based nanophotonic devices with unprecedented characteristics and unique functionalities. This field has been driven from multiple angles, including the expansion of available atomic-layered materials<sup>[28]</sup>, the impressive improvement in the techniques for assembling high-quality vdWHs with controlled thickness, sequence, and relative angles<sup>[29]</sup>, and the fast development of nano-optical characterization methods<sup>[6b, 7a, 30]</sup>. Exciting theoretical proposals have anticipated how these materials, when combined, can team up to produce new physical phenomena<sup>[28]</sup>. Furthermore, the electronic states of a large set of atomically thin 2D materials and their vdWHs have been mapped out<sup>[31]</sup>, thus assisting in the exploration of active modulation by chemical doping or electric gating. All of these factors have led to a dizzying growth in the complexity and functionality of vdWHs<sup>[32]</sup>, as exemplified by unconventional superconductivity<sup>[33]</sup>, exotic magnetism<sup>[34]</sup>, and generalized Wigner crystals<sup>[35]</sup>. Alongside these frontiers of vdWHs, exotic polariton features are expected to emerge from the behavior of their electronic, phononic, and excitonic degrees of freedom.

Here, we review the emerging but rapidly developing field of polaritons in vdWHs. Compared with the reviews on 2D material polaritons<sup>[6a, 14b, 14c, 20, 36]</sup>, we focus on the polaritons in vdWHs, and detailedly analyze the mechanisms of plasmons, phonon polaritons, and exciton polaritons in vdWHs which are classified depending on their macroscopic or microscopic characters in Section 2. We then separately review plasmons in vdWHs in Section 3, phonon and exciton polaritons in vdWHs in Section 4, and polariton hybridization in vdWHs in Section 5 to explore their unique properties. We conclude with a summary of challenges and perspectives opened by polaritons sustained by vdWHs in the field of nanophotonics.

Table 1. Diversity of already demonstrated polaritons in vdW heterostructures and opportunities remaining to be explored (indicated by ○). Numbers in the table indicate references.

Type of polariton		Plasmons	Phonon polaritons	Exciton polaritons	Cooper pair polaritons
<b>Tailoring mechanism</b>					
Macroscopic mechanism	Dielectric engineering	Phase change materials	○	[37]	○
		Dielectric designs	[38]	[3, 39]	[40]
	Coupling to optical structure	Optical cavities	[41]	[42]	[40b, 43]
		Resonant antennas	[44]	[45]	○
		Waveguides	[46]	[47]	[48]
		Photonic crystals / metasurfaces	[38]	[49]	[50]
Microscopic mechanism	Band structure engineering	Charge doping/transfer	[23, 51]	○	[52]
		Local strain/Moiré superlattices	[53]	[27a, 27d, 54]	[55]
		Molecular intercalation	[56]	[19]	○
	Coupling to other quasi-particle	Molecular vibrations	[14a, 14e]	[57]	○
		Cooper pairs	[8b]	○	○

S	Excitons	[58]	[58a]	○	○
	Plasmons	[8c, 41a, 41c, 44b, 53e, 59]	[4, 22b, 60]	[43d]	[13]
	Phonon polaritons	[4, 22b, 60]	[27, 54b, 61]	○	○
	Exciton polaritons	[40b]	○	○	○

## 2. Mechanisms of polariton modulation in vdWHs

We find it interesting to classify existing studies on 2D polaritons in vdWHs according to the macroscopic or microscopic mechanisms that are explored, as shown in Table 1. Indeed, plasmons, phonon, exciton, and cooper-pair polaritons have already been extensively studied in vdWHs. In general, they can be engineered and coupled via the following methods: (I) dielectric engineering of the environment, (II) coupling between polaritons and optical structures, (III) band-structure engineering of the materials supporting polaritons, and (IV) coupling between polaritons and other quasi-particles (i.e., polaritons, molecular vibrations, excitons and so on). **Figure 1** summarizes the main features of polaritons in vdWHs, including the operation mechanisms and main applications. Microscopic mechanisms correspond to band-structure engineering and coupling to quasi-particles, which are mainly achieved through charge doping and emergence of moiré superlattices in the vdWHs. Others macroscopic mechanisms are related to the electromagnetic coupling between polaritons and electromagnetic modes across layers and in the environment (i.e., dielectric response and nanostructure optical modes). Applications of the polaritons span a wide range including

# Accepted Article

communication and information technologies, quantum information, imaging, detecting and sensing, and energy harvesting.

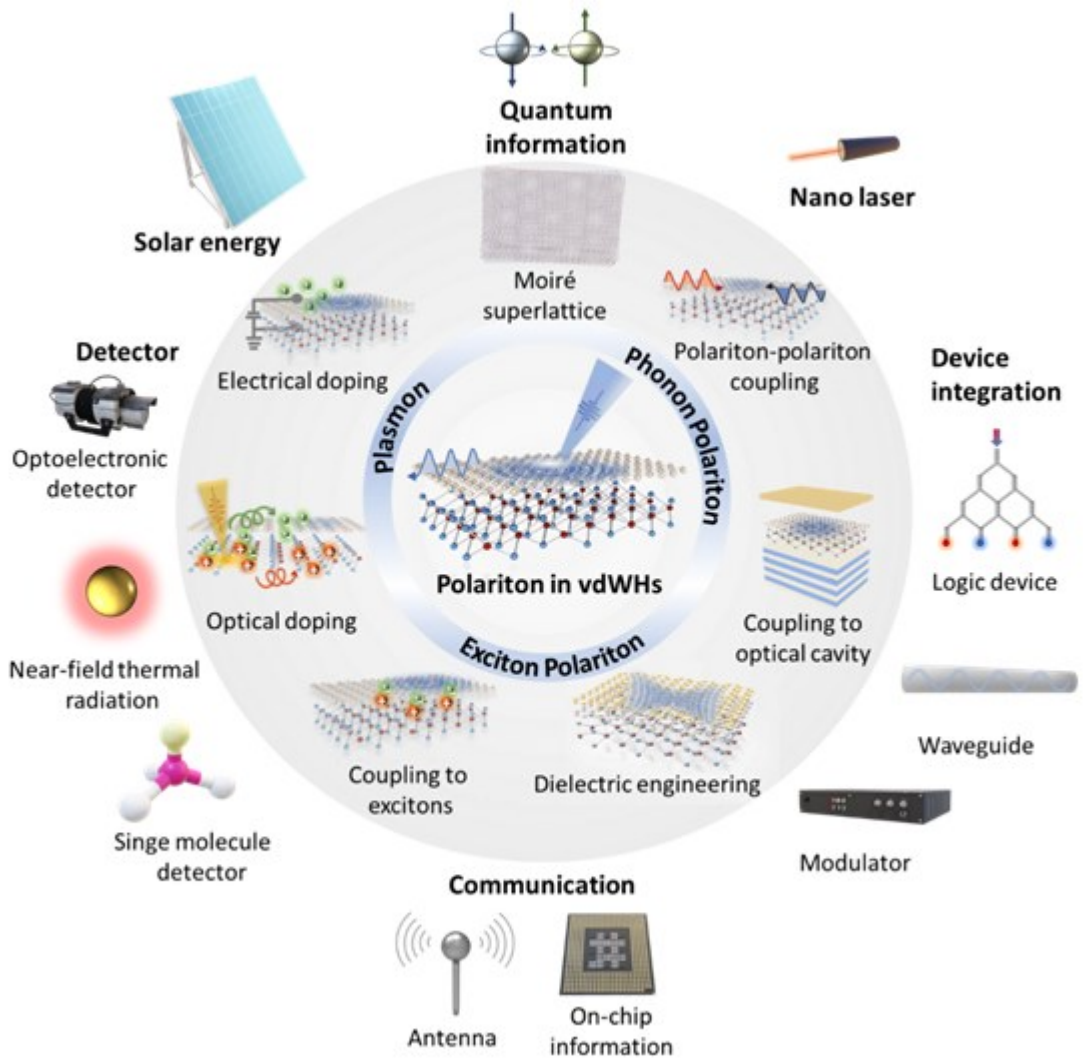


**Figure 1.** Polaritons of 2D materials in vdWHs: From fundamental properties to disruptive applications. Polaritons sustained by vdWHs feature widely tunable and distinct properties. Plasmons, phonon polaritons, and exciton polaritons can be tailored by relying on microscopic mechanisms (e.g., electrical doping, optical doping, coupling to other quasi-particles such as polaritons and excitons, and moiré superlattices) and macroscopic

mechanisms (e.g., dielectric engineering, coupling between polaritons and optical structures). These mechanisms have been exploited to realize integrated devices with wide applications.

### 3. Plasmons in vdWHs

Metallic and semiconducting 2D materials such as graphene and black phosphorus (BP) can support plasmons (the collective oscillation of free electrons aimed by their electromagnetic interactions). Plasmon properties mainly depend on the carrier density, carrier mobility, optical structure, and surrounding environment of the hosting materials. Even if the intrinsic plasmons of graphene and BP have excellent properties (e.g., tunability, low loss, and high confinement), stacking layers with distinct dielectric, electronic, optical, and magnetic properties can introduce novel and exciting functionalities<sup>[7a, 22a, 59b]</sup>, which are relevant to many plasmonic applications, such as sensitive detectors and efficient emitters. Next, we review several examples to discuss the involved mechanisms (ranging from microscopic to macroscopic) and the corresponding advantages.

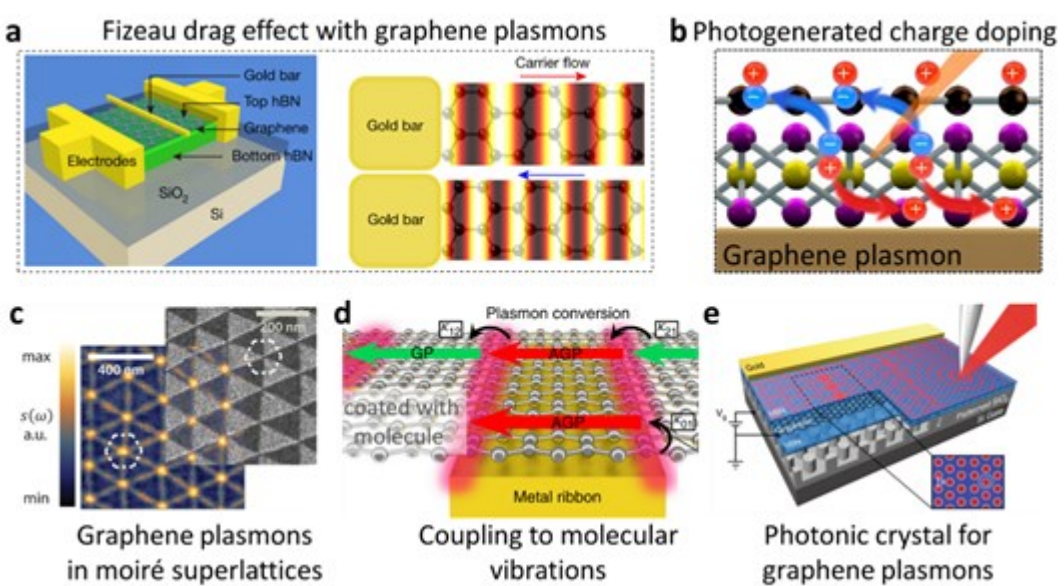


**Figure 2.** Plasmonic zoo in 2D vdWHs. (a) Efficient Fizeau drag of graphene plasmons from Dirac electrons in a gate-tunable h-BN/graphene/h-BN heterostructure<sup>[51d]</sup>. Copyright 2021, Springer Nature. (b) All-optical modulation of graphene plasmons via photogenerated charge doping in a graphene/monolayer MoS<sub>2</sub> heterostructure<sup>[23]</sup>. (c) Visualizing a nanoscale photonic crystal for graphene plasmons in twisted bilayer graphene<sup>[26]</sup>. Copyright 2018, Science. (d) Acoustic graphene plasmons of the graphene/Al<sub>2</sub>O<sub>3</sub>/Au heterostructure strongly coupling to molecular vibration modes<sup>[41c]</sup>. Copyright 2019, Springer Nature. (e) Graphene-plasmon photonic crystal formed by integrating a continuous graphene monolayer in a back-gated substrate with nano-structured gate insulators<sup>[38a]</sup>. Copyright 2019, Springer Nature.

### 3.1 Band structure engineering

#### 3.1.1 *Voltage-gated plasmonic devices with high quality*

Dynamical tuning of plasmons in 2D atomic crystals can be efficiently achieved through voltage-gated devices. Among all 2D materials, graphene and its plasmons are the most widely studied due to the low loss and dynamical tunability inherited from the linear Dirac dispersion of graphene. Its relatively low and tunable carrier density of this material renders graphene plasmons tunable from terahertz to mid-infrared frequencies, and even extending to the near infrared region. This is in contrast to surface plasmon polaritons of metals, which are typically emerging in the ultraviolet to the near-infrared range of frequencies. However, the first demonstrated voltage-gated graphene plasmonic devices fabricated on Si/SiO<sub>2</sub> substrates exhibited relatively modest plasmon lifetimes<sup>[8e, 8f, 22a]</sup> (<100 fs) as a result of low carrier mobility and high charge disorder produced by charged impurities and surface phonons in the SiO<sub>2</sub> dielectric substrate.

Eventually, by encapsulating graphene in h-BN/graphene/h-BN vdWHs, it was found that h-BN can act as an atomically flat dielectric free of dangling bonds, enabling devices with ultralow disorder that reduce losses and produce long plasmon lifetimes (~500 fs,

corresponding to  $\sim 9$  plasmon wavelengths of propagation distance<sup>[22a, 62]</sup>). This kind of vdWHs also introduce superb gate-voltage tunability. For example, electrical  $2\pi$  phase-shift control of infrared light was demonstrated in one of such vdWHs sustaining graphene plasmons with a 350-nm footprint<sup>[63]</sup>. The plasmon lifetime in h-BN/graphene/h-BN vdWHs can be further extended by eliminating impurity scattering in high-quality samples and going to cryogenic temperatures to dramatically reduce inelastic plasmon coupling to thermal phonons<sup>[7a]</sup>. Remarkably, the plasmon propagation length measured at liquid nitrogen temperature using scattering scanning near-field optical microscopy (s-SNOM) can exceed 50 plasmon wavelengths ( $\sim 10$   $\mu\text{m}$ , corresponding to 1.6 ps lifetime), which defines a record of highly confined and tunable polariton modes<sup>[7a]</sup>. Such high-quality modes open the exploration of quantum effects, such as the Fizeau drag of graphene plasmons, which was directly visualized in h-BN/graphene/h-BN vdWHs through s-SNOM imaging at 170 K<sup>[51c]</sup> and 25 K<sup>[51d]</sup>. Due to electron flow dragging during propagation of graphene plasmons, a plasmon wavelength difference of 3.6% can be introduced by a drag current relative to the situation without a current, as shown in **Figure 2a**.

Besides h-BN, other vdW materials, such as mica and 2D Talc<sup>[64]</sup>, have also been explored as atomically flat substrates for graphene plasmons. In graphene/mica vdWHs, not only the quality of graphene plasmons is improved, but also flexible plasmon devices can be made<sup>[64a]</sup>. Dual-gated graphene devices for near-field imaging were developed in the vdWHs of graphene/h-BN/graphene/h-BN, bilayer MoS<sub>2</sub>/h-BN/graphene/h-BN, and WSe<sub>2</sub>/h-BN/graphene/h-BN<sup>[51e, 65]</sup>.

### 3.1.2 Plasmon modulation through chemical and optical doping

Charge redistribution between adjacent layers in vdWHs can also be used to modulate plasmons with new functionalities. For example, robust plasmonic features were visualized in an undoped graphene/ $\alpha$ -RuCl<sub>3</sub> vdWH due to the massive charge transfer taking place at the

interface of graphene/α-RuCl<sub>3</sub><sup>[51a]</sup>. The graphene Fermi energy were evaluated to be about 0.6 eV, thus implying that vdWHs provide an efficient strategy for generating nanometer-scale plasmonic interfaces without resorting to external gating. Depositing ordered molecular layers of pentacene on top of a graphene layer can also modulate its plasmons<sup>[51b]</sup>. The plasmon wavelength decreases systematically, but nonlinearly, with the pentacene thickness due to the occurrence of tunneling-type electron transfer from pentacene to graphene<sup>[51b]</sup>. Unlike electrical gating, which requires an active bias voltage, these interface charge transfer methods provide a way to tailor graphene plasmons with permanent properties for long-term applications.

Photogenerated carrier transfer in vdWHs opens a new approach to all-optical modulation of plasmons in 2D materials. For example, efficient all-optical mid-infrared plasmonic modulators have been realized in graphene/monolayer MoS<sub>2</sub> vdWHs due to the ultrafast and efficient doping of graphene with the photogenerated carrier in monolayer MoS<sub>2</sub> (Figure 2b)<sup>[23]</sup>. The direct-gap in monolayer MoS<sub>2</sub> makes it possible to tune graphene plasmons by using a conventional light-emitting diode, while the fast interface charge transfer (~600 fs) in atomically thin vdWHs is highly promising for ultrafast plasmon modulation.

Chemical and optical doping modulation approaches can greatly extend the functionalities and applications of plasmons in 2D materials, which largely depend on the properties of the constituent layers. As such, this subfield can benefit from the development of new materials and the improvement in techniques for the fabrication of high-quality vdWHs. For example, some high-quality monolayer TMDs such as WSe<sub>2</sub> and WS<sub>2</sub> possess an even higher photosensitivity than MoS<sub>2</sub>, so they appear to be promising for application in graphene plasmon modulation.

### 3.1.3 Modifying plasmons through moiré patterns

In vdWHs, the lattice mismatch or rotational misalignment between stacked 2D layers can produce moiré superlattices in which the interlayer interactions qualitatively change the electronic band structure, generate new quantum phenomena, and strongly modify their plasmons. For example, moiré patterns formed due to minor lattice mismatch between graphene and h-BN have been widely studied, where tunable correlated insulating states, tunable superconductivity, mini-Dirac cones and the Hofstadter's butterfly patterns have been identified<sup>[66]</sup>. Infrared nano-imaging implies that the superlattice Dirac mini-bands in graphene/h-BN vdWHs can produce an additive contribution to the pristine graphene plasmon<sup>[53d]</sup>.

Moiré patterns formed in twisted bilayer graphene (TBLG) with small twist angles can act as natural plasmonic photonic crystals for controlling light at the nanoscale (Figure 2c)<sup>[26]</sup>. This is due to the periodic variations in the optical response of the vdWHs arising from the moiré domain walls<sup>[67]</sup>. The electronic structures across the moiré domain walls are topologically protected chiral one-dimensional (1D) states with enhanced local optical conductivity, which can support long-lifetime plasmons at room temperature<sup>[25]</sup> ( $\sim 3$  ps, exceeding monolayer graphene plasmon lifetimes encapsulated in h-BN,  $\sim 0.5$  ps<sup>[22a]</sup>). Plasmons supported by TBLG are extremely sensitive to the twist angle due to Fermi-velocity renormalization and its effect on interlayer electronic coupling<sup>[53f]</sup>.

In brief, these examples illustrate how these moiré vdWHs provide a pathway for controlling nanoscale light by exploiting the quantum properties of vdWHs<sup>[68]</sup>.

### 3.2 Plasmon coupling to other quasi-particles

Strong coupling between highly confined graphene plasmon and quasi-particles in several systems can be used in sensors and photodetectors. For example, in vdWHs consisting of graphene and a superconductor, the Higgs mode of the latter, which is usually challenging to observe through far-field optics, can be probed by coupling to graphene plasmons, giving rise

to a clear mode anticrossing<sup>[8b]</sup>. Likewise, coupling of graphene plasmons to molecular vibrations allows us to perform enhanced infrared spectroscopy for label-free identification of trace molecules<sup>[14c, 14d, 41c]</sup>. Additionally, using acoustic graphene plasmons with extremely high confinement, ångstrom-thick protein and SiO<sub>2</sub> layers can be sensitively detected via infrared spectroscopy (Figure 2d), providing a new platform for achieving strong light-matter interaction<sup>[41c]</sup>. Incidentally, a framework combining density functional theory (DFT) with macroscopic quantum electrodynamics (QED) has been developed for studying quantum light-matter interactions of intersub-band transitions in TMDs and acoustic polaritons<sup>[58b]</sup>.

### 3.3 Designing plasmons with optical structures and dielectrics

In graphene/dielectric/metal configurations, acoustic graphene plasmons with extremely high field confinement can be excited, so that light is vertically confined (as propagating plasmons) between the metal and the graphene<sup>[41a, 41c, 41d, 69]</sup>. These so-called acoustic plasmons originate from the strong hybridization of graphene plasmons with their mirror images in the metal layer<sup>[41c, 41d]</sup>, and they can exist even using monolayer h-BN as the dielectric (corresponding to a vertical confinement limit)<sup>[59b]</sup>. Besides, by using a silver nanocube as the metal in the graphene/monolayer h-BN/metal vdWHs, it has been shown that a single nanometer-scale acoustic graphene plasmon cavity is realized, reaching mode volume confinement factors of  $\sim 5 \times 10^{-10}$ <sup>[8c]</sup>. Acoustic plasmons in graphene/h-BN/metal vdWHs provide a platform for studying ultrastrong-coupling phenomena and have been explored for applications such as enhanced infrared spectroscopy<sup>[41c]</sup>, enhanced third-harmonic generation<sup>[24]</sup>, and probing the quantum surface-response functions of neighboring metals<sup>[41b]</sup>. Interestingly, the slow plasmon propagation velocity ( $c/250$ , close to the electron Fermi velocity) accompanied by the ultrahigh compression of light can be used to probe the nonlocal response of the graphene electron liquid<sup>[69]</sup>.

The direct combination of graphene and metal antennas are important for efficient excitation and emission of plasmons<sup>[44b]</sup>, which can find applications in optoelectronics, nanophotonic integrated circuits, sensing, and quantum information among others. For example, resonant optical antennas and designed metal patterns can be used for launching and controlling the propagation of graphene plasmons<sup>[70]</sup>. In this context, mid-infrared radiative emission from bright hot plasmons in graphene was observed by using gold nanodisks to promote scattering and localized plasmon excitation<sup>[44a]</sup>.

Periodically doped graphene can be realized by an integrating graphene layer with nanostructured gate insulators, providing an alternative method to control graphene plasmons. Using this approach, a tunable photonic crystal for graphene plasmons was realized by using a back-gated platform with nano-structured gate insulators (patterned SiO<sub>2</sub>)<sup>[38a]</sup>, as shown in Figure 2e. In the resulting plasmonic crystal structure, propagating plasmons with a continuous dispersion are transformed into Bloch polaritons that are programmable through the applied gate voltage<sup>[38b]</sup>. Moreover, for specific patterns of the gate and bias voltages, graphene-plasmon valleytronics are predicted theoretically<sup>[71]</sup>.

#### 4. Phonon and exciton polaritons in vdWHs

##### 4.1 Tuning phonon polaritons in vdWHs

The anisotropic features of 2D vdW materials such as h-BN and  $\alpha$ -MoO<sub>3</sub> endow their hyperbolic phonon polaritons (HPhPs) with extremely high confinement, which coupled to their ultralow inelastic losses have understandably attracted a wide interest in the research community<sup>[6b, 7c, 7d, 9, 72]</sup>. However, the difficulty in modifying the lattice vibrations of crystals makes it challenging to tune phonon polaritons. Constructing vdWHs provides a viable

approach to modulate and extend the functionalities of HPhPs in 2D crystals via the following mechanisms, ranging from macroscopic to microscopic in character.

#### 4.1.1 Dielectric engineering

The highly confined HPhPs sustained by 2D materials are very sensitive to the local dielectric environment. For example, the HPhPs in h-BN thin films or antennas can be modulated by placing it on different polar substrates, such as quartz, 4H-silicon carbide and gold film<sup>[39e, 73]</sup>, or covering it with layers of a high-refractive-index van der Waals crystal (WSe<sub>2</sub>)<sup>[39f]</sup>. The use of anisotropic substrates translates into anisotropic HPhPs, for example, when combining the in-plane isotropic HPhPs waveguide modes of h-BN with anisotropic BP in an integrated structure (**Figure 3a**)<sup>[39b]</sup>. Active tuning of the polaritonic resonances can be achieved using a gated graphene monolayer as the dielectric<sup>[39f, 74]</sup>.

Phase-transition materials, which can undergo dramatic changes in their optical behavior (e.g., insulator-metal transition) driven by external stimuli (e.g., temperature, stress, and optical pumping), provide a platform for HPhPs modulation<sup>[75]</sup>. For example, h-BN HPhPs can be dynamically modulated by varying the temperature (e.g., a 1.6-fold change of wavelength) when supported on a VO<sub>2</sub> substrate that transitions from dielectric to metallic in the range of 60 °C to 80 °C, which can also be used to design patterned local dielectric environments for the control of HPhPs propagation (Figure 3b)<sup>[37a, 37c]</sup>. In a parallel effort, by using the low-loss phase change material Ge<sub>3</sub>Sb<sub>2</sub>Te<sub>6</sub> to control HPhPs at the nanoscale, polariton refractive and meta-optics of h-BN HPhPs were also experimentally demonstrated<sup>[37b]</sup>.

Another rising type of vdWH structure to support ultraconfined surface phonon polaritons (SPhPs) comprises atomically thin vdW dielectrics (e.g., TMD<sup>[76]</sup> and MoO<sub>3</sub><sup>[39a]</sup>) supported on bulk dielectric (e.g., SiC, AlN, and GaN). In contrast to polaritons in 2D materials like h-BN, the polar substrate serves as a source of surface-phonon polaritons

(SPhPs), which are then confined into the atomic thin vdW dielectrics with a large confinement factor ( $>100$ )<sup>[76]</sup>. These ultraconfined SPhPs propagating in the atomic vdW materials can further be reconfigured and engineered by introducing anisotropic vdW materials and patterned substrates<sup>[39a]</sup>.

The high sensitivity of HPhPs to the dielectric environment can be used for nanoimaging nanostructures placed beneath the vdW materials (e.g., in buried or encapsulated device geometries). In this direction, the enlarged imaging and the super-resolution focusing of buried metallic nanostructure were demonstrated by using h-BN HPhPs<sup>[77]</sup>. Recently, the moiré superlattices of undoped twisted graphene bilayers encapsulated by h-BN were directly imaged through s-SNOM, which senses the effective optical phase change of the h-BN HPhPs reflectance at the domain walls and does not require the excitation of graphene plasmons<sup>[3]</sup>.

#### 4.1.2 Coupling via optical structures

Integrating HPhPs with optical structures in vdWHs can also generate high-quality hybrid polaritons. For example, phonon-polaritonic crystals were realized by incorporating h-BN film on a silicon-based photonic crystal, and local field distribution patterns resembling the Archimedean-like tiling were observed (Figure 3c)<sup>[49b]</sup>. Additionally, in a h-BN/dielectric/metal structure, ultraconfined acoustic HPhPs similar to acoustic plasmons can be generated due to the coupling between HPhPs and the image-potential response from the metal<sup>[61]</sup>. Also, by coupling to resonant metal plasmonic antennas, one can efficiently launch HPhPs in thin h-BN slabs<sup>[45b]</sup>, and the resulted enhanced light-matter interaction can be used for sensitive and fast mid-infrared photodetection based on graphene<sup>[45a]</sup>.

The vdWHs can also extend the functionalities of optical devices. For example, a h-BN/silicon hybrid waveguide can simultaneously enable dual-band operation at both mid-infrared and telecom frequencies<sup>[47]</sup>.

#### 4.1.3 Band structure and strain engineering

In vdWHs, rotational misalignment or lattice mismatch of the constituent layers gives rise to moiré superlattices, which can introduce periodic lattice strain (also denoted solitons in this context) to tune phonon polaritons (Figure 3d)<sup>[54b]</sup>. In addition, heating may further cause lattice strain due to the mismatch of the thermal expansion coefficients in different materials forming part of the vdWH. For example, for h-BN (negative expansion coefficient) on a silicon substrate (positive coefficient), wrinkles are generated in h-BN flakes after annealing, and consequently, strain causes blue shifts in the h-BN phonons and reduces the IR response below the resonance phonon frequency<sup>[54a]</sup>.

Molecule/atom intercalation can directly modify the HPhPs material, providing a novel method to chemically manipulating HPhPs. Specifically, intercalation of Na atoms in  $\alpha$ -V<sub>2</sub>O<sub>5</sub> enables a broad spectral shift of Reststrahlen bands, and the HPhPs show ultra-low losses (lifetime of  $4 \pm 1$  ps), similar to phonon polaritons in a non-intercalated crystal (lifetime of  $6 \pm 1$  ps)<sup>[19c]</sup>. Additionally, switching of HPhPs in  $\alpha$ -MoO<sub>3</sub> can be achieved through non-volatile and recoverable hydrogen intercalation (Figure 3e)<sup>[7c, 19b]</sup>. Moreover, efficient and tunable reflection of HPhPs were demonstrated at the built-in intercalation interfaces<sup>[19a]</sup>.

#### 4.1.4 Coupling to molecular vibrations

The ultra-strong coupling observed between HPhPs and molecular vibrations is not only a new method to modulate phonon polaritons, but it also suggests that phonon polaritons can be utilized for molecule recognition. More precisely, strong coupling between HPhPs in h-BN and molecular vibrations in adjacent molecular layers causes the emergence of pronounced mode anti-crossing patterns in the dispersion relations (Figure 3f)<sup>[57a]</sup>. Likewise, HPhPs in h-BN nanoresonators have also been demonstrated to enhance molecular vibrational spectroscopy, reaching the strong coupling limit<sup>[57b]</sup>.

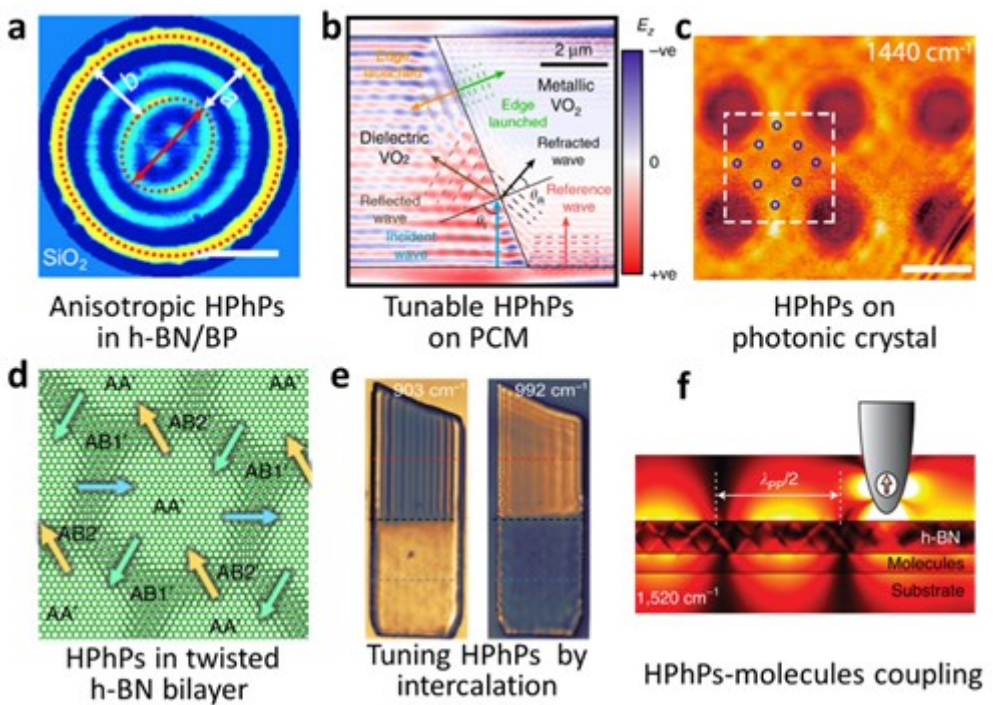


**Figure 3.** Phonon polaritons of 2D materials in vdWHs. (a) Scattering SNOM image of anisotropic HPhPs modes (frequency  $\omega=1410\text{ cm}^{-1}$ ) in a h-BN/BP heterostructure<sup>[39b]</sup>. Scale bars, 2  $\mu\text{m}$ . (b) Refraction of h-BN HPhPs within a h-BN/VO<sub>2</sub> vdWH at the domain boundary of dielectric and metallic VO<sub>2</sub><sup>[37c]</sup>. (c) Photonic crystal for h-BN HPhPs made by integrating a h-BN flake on a silicon optical crystal<sup>[49b]</sup>. Scale bar, 2  $\mu\text{m}$ . Copyright 2021, American Chemical Society. (d) Schematic diagram of a soliton superlattice in a twisted h-BN bilayer<sup>[54b]</sup>. (e) Tuning of  $\alpha\text{-MoO}_3$  HPhPs by intercalation with hydrogen (the black dashed line indicates the hydrogenation boundary)<sup>[19b]</sup>. (f) Strong coupling between propagating HPhPs in h-BN and molecular vibrations in an adjacent thin molecular layer<sup>[57a]</sup>. Copyright 2020, Springer Nature.

#### 4.2 Exciton polaritons in vdWHs

Exciton polaritons with low effective mass and strong nonlinearity in atomically thin crystals offer an ideal platform for studying Bose-Einstein condensation, superfluidity, soliton transmission, quantum vortex effects, and other fundamental phenomena. Moreover,

materials sustaining exciton polaritons are compatible with a wide range of substrates and optoelectronic device geometries, therefore enabling new strategies to control high-quality exciton polaritons by engineering vdWHs.

#### 4.2.1 *Integration in optical structures*

By integrating monolayer TMDs (e.g., MoS<sub>2</sub><sup>[78]</sup>, WS<sub>2</sub><sup>[43f, 79]</sup>, MoSe<sub>2</sub><sup>[80]</sup>, and WSe<sub>2</sub><sup>[81]</sup>) with high-quality-factor optical cavities or antennas one can reach the strong light-matter coupling regime and form hybrid exciton polaritons<sup>[78, 82]</sup>. Specifically, room temperature exciton polaritons were observed in monolayer TMDs embedded in a dielectric Fabry–Perot (FP) microcavity due to the high quantum yield and large exciton binding energy monolayer<sup>[78, 81–82]</sup>. Recently, compelling evidence of bosonic condensation of exciton polaritons has been found in an atomically thin crystal of MoSe<sub>2</sub> embedded in a dielectric microcavity under optical pumping at cryogenic temperatures (**Figure 4a**)<sup>[83]</sup>. In addition, spin- and valley-selective propagation of exciton polaritons was observed in a monolayer of MoSe<sub>2</sub> that was strongly coupled to a microcavity photonic mode<sup>[43c]</sup>.

Optical structures such as compact Tamm-plasmon photonic microstructure (Figure 4b)<sup>[82a]</sup>, open cavities<sup>[43d, 43f, 84]</sup>, metasurfaces<sup>[50b]</sup>, and photonic crystal structures<sup>[50a, 85]</sup> have also been demonstrated to couple with TMDs to form 2D exciton polaritons, thus opening a way for developing novel and exotic exciton-polariton devices. For example, helical topological polaritons were found to survive up to 200 K without any external magnetic field in monolayer WS<sub>2</sub> excitons coupled to a nontrivial hexagonal photonic crystal protected by pseudo time-reversal symmetry (Figure 4c)<sup>[50a]</sup>. Highly nonlinear trion-polaritons were also observed in monolayer TMDs<sup>[84a]</sup>.

#### 4.2.2 *Charge carrier manipulation*

vdWHs additionally enable new strategies for tuning exciton polaritons by controlling light-matter coupling and carrier doping/injection. For example, spatially separated indirect excitons with ultralong lifetime can be produced by the coupling between partially filled Landau levels in the quantum-Hall-effect region of double-bilayer-graphene/h-BN vdWHs (Figure 4d)<sup>[52c]</sup>. High-temperature exciton condensation was also observed in electrically generated interlayer excitons in MoSe<sub>2</sub>-WSe<sub>2</sub> double atomic layers with a density up to 10<sup>2</sup> excitons per square centimeter<sup>[86]</sup>. These vdWHs provide an ideal platform for exploring the strong bosonic behavior regime in electronic systems. Moreover, the cavity spectroscopy of monolayer MoSe<sub>2</sub> can be electrically tuned (e.g., in a vdWH consisting of MoSe<sub>2</sub>/h-BN/graphene) and exhibits strongly bound trion and polariton resonances, as well as nonperturbative coupling to a single microcavity mode (Figure 4e)<sup>[52b]</sup>.

#### 4.2.3 Moiré polaritons in twisted vdWHs

Moiré lattice potentials formed in vdWHs can tune the properties of excitons. Recently, by integrating MoSe<sub>2</sub>-WS<sub>2</sub> heterolayers in a microcavity, a cooperative coupling between moiré-lattice excitons and microcavity photons was obtained up to the temperature of liquid nitrogen (Figure 4f), thereby integrating versatile control of both matter and light into one platform to study collective phenomena<sup>[55]</sup>.

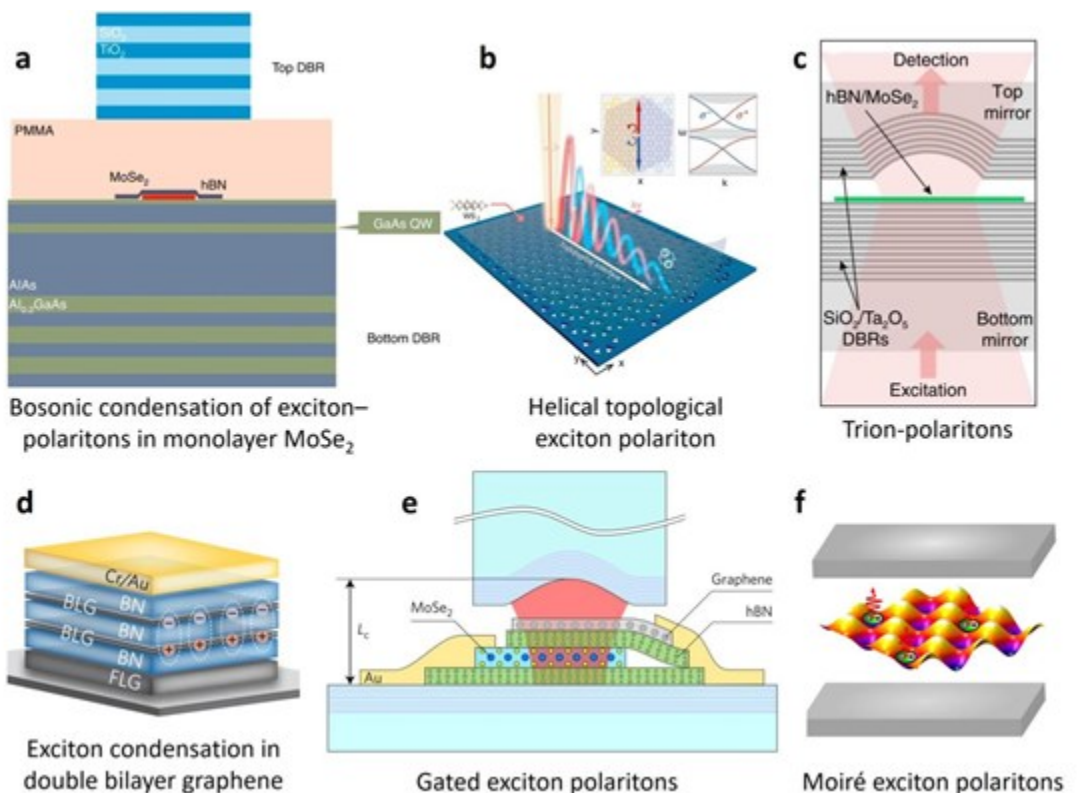


**Figure 4.** Exciton-polaritons in vdWHs. (a) Bosonic condensation of exciton–polaritons in MoSe<sub>2</sub>/h-BN vdWHs integrated with top and bottom DBR<sup>[83]</sup>. Copyright 2021, Springer Nature. (b) Helical topological exciton polariton by coupling a monolayer of WS<sub>2</sub> to a nontrivial photonic crystal<sup>[50a]</sup>. Copyright 2020, Science. (c) h-BN/MoSe<sub>2</sub> monolayer placed in an open-access microcavity where Laguerre–Gauss photonic modes strongly couple to exciton and trion states forming polaritons<sup>[84a]</sup>. (d) Exciton condensation in two bilayer graphene systems where interlayer excitons are created in the quantum Hall region<sup>[52c]</sup>. Copyright 2017, Springer Nature. (e) Gated exciton-polaritons in the MoSe<sub>2</sub>/h-BN/graphene heterostructure<sup>[52b]</sup>. Copyright 2016, Springer Nature. (f) Schematic of the moiré polariton system formed by excitons confined in a moiré lattice and coupled to a planar optical cavity<sup>[55]</sup>. Copyright 2021, Springer Nature.

## 5. Polariton-polariton coupling in vdWHs

In vdWHs, the vertical stacking of different polaritonic materials can result in strong coupling between different types of polaritons, opening up an exciting perspective to modulate and design polaritonic devices.

### 5.1 Plasmon-plasmon coupling

In graphene/dielectric/metal vdWHs, acoustic graphene plasmons with extremely high confinement can be excited due to the hybridization between graphene plasmons and their image-potential plasmons in the metal (**Figure 5a**)<sup>[59b]</sup>, as discussed above in Sec. 3.3. Plasmon-plasmon interactions in graphene/spacer/graphene<sup>[87]</sup> and graphene/spacer/BP vdWHs have been studied and shown to cause a redistribution of the plasmonic field depending on both the involved materials and the structure parameters<sup>[59c]</sup>. Moreover, in a mixed-dimensional single-walled carbon nanotube/h-BN/graphene vdWHs, the hybrid of 1D and 2D plasmons can retain the high figures of merit of 1D plasmons and additionally have the gate tunability<sup>[88]</sup>.

In the context of twisted photonics, coupling and hybridization between graphene plasmons has also been investigated. In particular, as shown in Figure 5b, when two layers of graphene nanoribbons are stacked with a misalignment angle, the hybridization of hyperbolic polaritons that are supported by the graphene nanoribbon layers undergo a transition through an optical topological state as the angle is varied<sup>[89]</sup>.

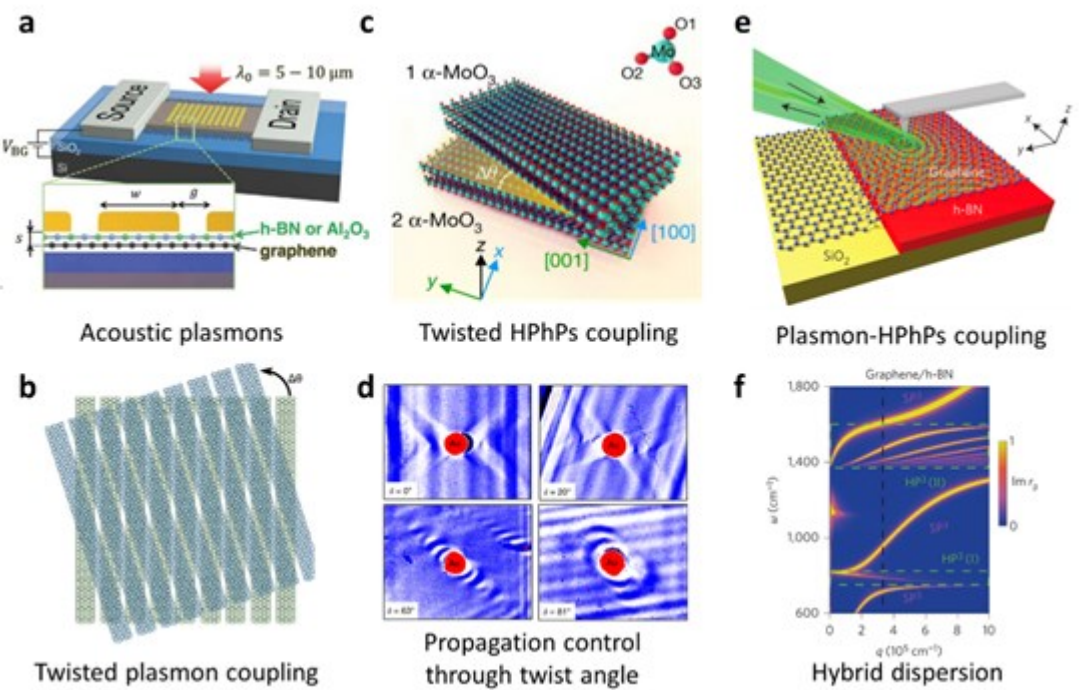


**Figure 5.** Polariton-polariton coupling in vdWHs. (a) Ultraconfined acoustic plasmons generated by the coupling of graphene plasmons and image interaction in the metal in a gold nanoribbon/dielectric/graphene vdWH<sup>[59b]</sup>. Copyright 2018, Science. (b) Plasmon-plasmon coupling in twisted hyperbolic metasurface (graphene nanoribbon arrays) stacked with a twist angle<sup>[89]</sup>. Copyright 2020, American Chemical Society. (c) Schematic of twisted  $\alpha\text{-MoO}_3$  layers<sup>[27a]</sup>. Copyright 2020, Springer Nature. (d) HPhPs-HPhPs coupling (s-SNOM amplitude images) in twisted  $\alpha\text{-MoO}_3$  controlled through the twisting angle ( $0^\circ, 20^\circ, 63^\circ$ , and  $90^\circ$  in the images)<sup>[27b]</sup>. Copyright 2020, Springer Nature. (e) Plasmon-HPhPs coupling in a graphene/h-BN vdWH<sup>[4]</sup>. Copyright 2015, Springer Nature. (f) Dispersion of hybridized plasmon-HPhPs<sup>[4]</sup>. Copyright 2015, Springer Nature.

## 5.2 Coupling between phonon polaritons

In-plane anisotropic crystal layers such as  $\alpha\text{-MoO}_3$  can support HPhPs that are of course anisotropic in the basal plane<sup>[7c, 7d]</sup>. These types of modes can generate abundant exotic phenomena by coupling with each other or with traditional HPhPs. For example, twisted

$\alpha$ -MoO<sub>3</sub> vdWHs (Figure 5c) have been designed to manipulate the propagation direction of HPhPs (Figure 5d) via the introduction of a twisting angle<sup>[27]</sup>. To achieve efficient control, the twisting configuration requires: (1) extreme basal plane anisotropy of the polaritons; (2) sufficient overlap of the polariton fields from stacked slabs<sup>[27b]</sup>. Both are actually advantageous properties provided by vdWHs.

Hybrid polaritons can also be produced in the  $\alpha$ -MoO<sub>3</sub>/SiC heterostructure at their common phonon-polaritonic frequency range. When anisotropic HPhPs of  $\alpha$ -MoO<sub>3</sub> meet the isotropic SiC phonon polaritons, the iso-frequency curves of the resulting hybrid polaritons undergo a topological change due to the presence of strong coupling and unique coupling characteristics. Interestingly, this behavior dramatically changes the propagation of  $\alpha$ -MoO<sub>3</sub> HPhPs, from previously forbidden transmission directions into newly possible transmission directions<sup>[39a]</sup>.

It should be noted that, although the methodology for tuning phonon polaritons in twisted  $\alpha$ -MoO<sub>3</sub> is similar to that for twistronics in moiré engineering<sup>[54b]</sup>, their physical origins are different. The former stems from the angle-dependent electromagnetic hybridization between anisotropic HPhPs in stacked  $\alpha$ -MoO<sub>3</sub><sup>[27b]</sup>, whereas the latter is attributed to the peculiar strain engineering by vdW superlattices<sup>[54b]</sup>.

### 5.3 Hybridization between plasmons and phonon polaritons

Since plasmons in the mid-infrared range can cover the frequency band of HPhPs, electromagnetic coupling between plasmons and phonon polaritons should allow them to combine their advantages. As an instance of such type of hybrid modes, phonon-plasmon polaritons in graphene/h- BN heterostructures are signaled by band anti-crossings in the graphene plasmon dispersion near the energy of h-BN optical phonons (Figure 5e,f)<sup>[90]</sup>. Such hybridized modes combine the long lifetime of HPhPs and the tunability of graphene plasmons<sup>[4, 22b, 91]</sup>. Moreover, when the isotropic graphene plasmons is replaced by in-plane

anisotropic BP plasmons, anisotropic plasmon-phonon-polariton modes are observed in the BP/h-BN vdWHs<sup>[92]</sup>. All-angle in-plane negative refraction between plasmons, phonon polaritons, and their hybrid polaritons in vdWHs have been predicted based on full-wave simulations, which can be used for the design of nanoscale metasurfaces and nanoimaging elements<sup>[5, 93]</sup>. In addition, hybrid modes in graphene/h-BN vdWHs can be combined with other types of structures, such as air-Au microstructured substrates, to further control the direction and velocity of polariton propagation<sup>[60a]</sup>.

## 6. Perspectives

Although the study of polaritons in vdWHs is still in its infancy, vdWHs offer exciting opportunities for designing high-quality 2D polaritons based on the vast and expanding family of 2D materials and the ability to arbitrarily program new stacked structures. We therefore anticipate that atomically thin vdW materials and their ultraconfined polaritons are promising for the miniaturization and integration of optoelectronic devices. Therefore, polaritons in vdWHs can provide an effective solution to the ultimate goal of optoelectronic on-chip integration, thus breaking the limitations associated with Moore's law in silicon-based chips. Here, we present an outlook on functional on-chip integrated devices in **Figure 6a**, including nanoscale light sources (optical and electrical excitation in Figure 6b,c), optical waveguides (polariton waveguides at telecom wavelengths with controllable transmission in Figure 6d,e), optical modulator and switches (from modulator to quantum computing in Figure 6f,g), detectors (single-molecule infrared detection, miniature infrared spectrometer, near-field thermal detection in Figure 6h-j), and others.

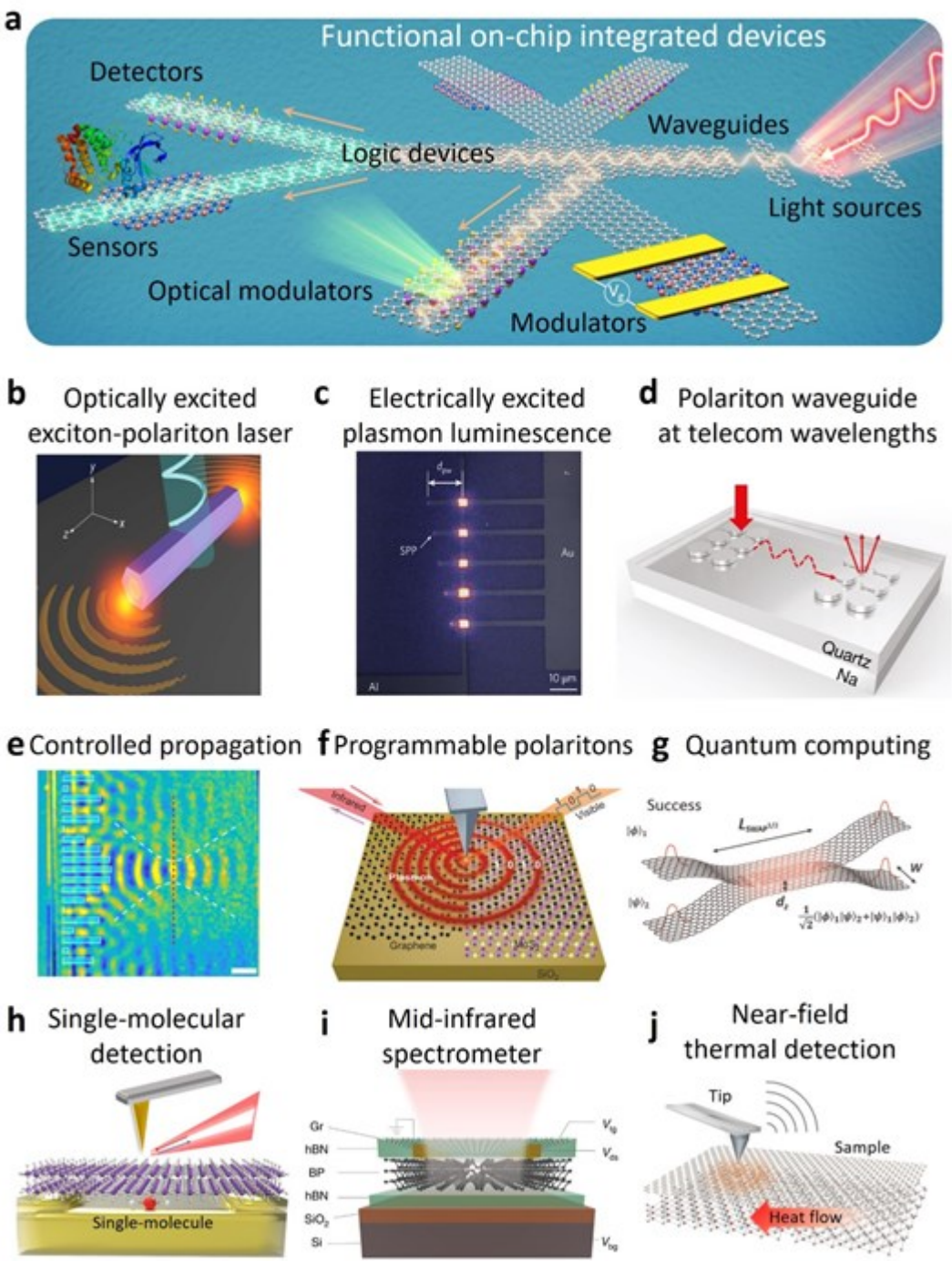


**Figure 6.** On-chip polaritonic devices based on vdWHs. (a) Schematic diagram of the photonic integrated devices and a photonic integrated circuit in the vdWHs. (b) Schematic

illustration of a single nanorod exciton polariton laser driven by optical excitation<sup>[94]</sup>. (c) Electrically excited plasmon luminescence in a gold nanostructure<sup>[95]</sup>. Copyright 2017, Springer Nature. (d) Telecom polariton on sodium-based plasmonic waveguiding nanostructure<sup>[96]</sup>. Copyright 2020, Springer Nature. (e) Controlled propagation of phonon polaritons in h-BN on the phase-change material  $\text{Ge}_3\text{Sb}_2\text{Te}_6$ <sup>[37b]</sup>. (f) Programmable polaritons in a monolayer  $\text{MoS}_2$ /graphene vdWHs<sup>[23]</sup>. (g) Quantum computing with graphene plasmons<sup>[97]</sup>. (h) Infrared single-molecule detection with acoustic polaritons<sup>[98]</sup>. Copyright 2021, Royal Society of Chemistry. (i) Ultrasmall mid-infrared spectrometer<sup>[99]</sup>. Copyright 2021, Springer Nature. (j) Detection of near-field heat flux.

## 6.1 Light/polariton sources

*Optically excited exciton-polariton lasers.* Polariton condensates have broad prospects to design energy-efficient lasers. However, in order to produce useful laser applications, we need to meet three core requirements: coherence, room-temperature operation, and electrical injection of charge carriers. In a polariton laser (Figure 6b), the coherence of the emitted radiation is inherited from the condensate wave function<sup>[94]</sup>. Then, layers of TMDs have been identified as a promising platform for this purpose, with the potential of operating at elevated temperatures<sup>[100]</sup>. However, it remains a technical challenge to reliably implement carrier electrical injection in a material system that holds large exciton binding energy. Hybrid inorganic-organic devices and electrically pumped TMD heterostructures could become a visionary route to overcome such current limitations<sup>[78]</sup>.

*Electrically excited polaritons.* Usually, polaritons are excited by light sources and after travelling along a waveguide, they are re-emitted as photons into free space. For practical applications of polaritons in integrated circuits, there is a need to generate and read out polariton signals by direct electrical means, without involving the intermediate generation of excitons, as shown in Figure 6c<sup>[95]</sup>. The coupling of metal-insulator-metal (MIM) tunnel junctions to polariton waveguides provides an effective way for electronic-polariton

transducers. MIM vdWHs have the advantage of atomic-scale thickness and provide a promising platform to integrate such reading electronic devices with polariton waveguides.

## 6.2 Optical waveguides

*2D polaritons at the telecom frequency.* To cope with the ever-growing demand for higher data-transfer rates, broader bandwidths, and higher on-chip integrability in telecommunication applications, highly confined 2D polaritons at the telecom frequency range are needed (Figure 6d)<sup>[96]</sup>. However, the widely studied families of 2D polaritons provided by graphene plasmons and h-BN HPhPs operate at frequencies below the telecom frequency range<sup>[6b, 23]</sup>. The variety and complexity of vdWHs are promising to realize 2D polaritons in the telecom frequency range by choosing appropriate materials<sup>[101]</sup> and stacking factors for telecom applications, such as data interconnection, light sources, modulators, and detectors. The combination of more conventional dielectric waveguides with tuning elements based on doped graphene and electrically shifted excitons also appears as a promising approach to actively controllable telecom waveguides.

*Controlled propagation of polaritons.* Manipulating high-speed and low-loss photonic circuits at the nanoscale has become a goal pursued in the field of polariton. The most effective means to manipulate polariton propagation are designing dielectric environment in a heterojunction system, such as 2D materials on photonic crystals<sup>[50a, 102]</sup>, on phase change materials<sup>[37b, 37c, 39d]</sup> and on other substrates<sup>[39a, 103]</sup>. With the development of optical nanostructures and active materials, the optical field will be greatly manipulated to realize prototype devices such as in-plane metalenses (e.g. Figure 6e)<sup>[37b]</sup>. In addition, the unidirectional propagation of polariton can also be manipulated by means of a one-dimensional grating structure<sup>[104]</sup>, which provides a new dimension to control the polariton propagation.

## 6.3 Optical modulators and logic gates

*Modulators.* Modulators superimpose information signal onto carrier signal for the purpose of light communication, which should obviously benefit from the availability of a wide range of actively tunable polaritons in vdWHs<sup>[36a]</sup>. 2D polaritons are much easier to be modulated than modes in conventional 3D structures because the electronic states of the constituent atomic layers are fully exposed to the chosen external stimuli. More importantly, the rich materials and stacking structures in vdWHs demonstrate the flexibility and diversity of polariton modulation (e.g, electrical/optical/chemical doping (Figure 6f)<sup>[7a, 8c, 23, 60c, 105]</sup>, temperature<sup>[37a, 37c]</sup>, and mechanical strain). Moreover, twisted vdWHs have showcased interesting features, including flexibility and tunability in manipulating light, contributing to the novel photonic devices<sup>[26]</sup>.

*Quantum logic gates.* Among the various approaches to quantum technologies (e.g., computing, communication, imaging, and sensing), all-optical architectures are especially promising due to the robustness and mobility of single photons<sup>[106]</sup>. A universal two-qubit logic gate, where qubits are encoded as surface plasmons propagating along graphene nanostructures, exploiting the strong third-order nonlinearity and long plasmon lifetimes in this material, has been proposed to enable single-photon-level interactions (Figure 6g)<sup>[97]</sup>. In particular, strong two-plasmon absorption in graphene nanoribbons can greatly exceed single-plasmon absorption to create a *square-root-of-swap* that is protected by the quantum Zeno effect against the evolution into undesired failure modes.

#### 6.4 Detectors

*Single molecule identification.* Ultraconfined polaritons in vdW materials have demonstrated the compression of infrared light into nanoscale volumes, which can largely enhance light-matter interaction to facilitate molecule sensing and identification. In particular, graphene-enabled ultrasensitive detection has recently been demonstrated for biological and inorganic molecules<sup>[41c]</sup>. By designing polaritonic vdWHs with atomically thin nanocavities,

the ultimate limits of light confinement could be explored, which could potentially contribute to reach the sought-after detection limit of single molecules (see Figure 6h)<sup>[98]</sup>.

*Ultrasmall mid-infrared spectrometers.* Optical spectrometry is one of the most powerful and widely used characterization tools in scientific and industrial research. Spectrometers are cornerstone instruments in scientific research across various disciplines and in technological developments for many industries<sup>[99]</sup>. However, the demand for portable or handheld spectral analysis devices (Figure 6i) requires shrinking of these systems down to centimeter-scale footprints<sup>[107]</sup>. With the strong light-matter interaction, multifunctionality, and ultracompact integration offered by polaritons in vdWHs, ultrasmall single-detector spectrometers should have extraordinary potential in reconstructing the spectrum of broadband light with unparalleled speed and sensitivity.

*Enhanced near-field thermal detection.* Ultraconfined polaritons in 2D materials feature a high density of optical energy, which can significantly enhance near-field thermal detection beyond the diffraction limit (Figure 6j). In particular, graphene plasmons, h-BN HPhPs, and their hybridized polariton modes in vdWHs have demonstrated to yield super-Planckian heat transfer, which for some engineered designs can become the leading mechanism of heat dissipation<sup>[108]</sup> (i.e., faster than even conventional heat diffusion). Therefore, polaritons in vdWHs can be used as a good platform to study the physical mechanisms of near-field thermal radiation and develop new thermal management devices (i.e., heat-assisted magnetic recording, thermal lithography, scanning thermal microscopy, non-contact thermal management, thermal circuits, and near-field thermophotovoltaics).

In conclusion, this review shows that vdWHs based on the combination of 2D materials have greatly improved our ability to manipulate polaritons, and consequently, these types of structures have expanded our capabilities for new applications at the frontiers of nanoscale photonics and optoelectronics. We expect that polaritons in vdWHs will play a major role in

promoting the development of many advanced interdisciplinary studies addressing nano-optoelectronic devices, nano-energy devices, and nano-biological devices to name a few.

## **Box 1: Fundamentals of polaritons and vdWHs**

### **2D polaritons**

Polaritons are quasiparticles sustained by a material as a result of the interaction and mixing between light and polarization charges (i.e., dipole active transitions) in the medium. In particular, surface polaritons can be excited as surface electromagnetic waves at the interface between positive (e.g., air or a conventional dielectric) and negative (e.g., two-dimensional van der Waals (2D vdW) structures) permittivity materials<sup>[6a]</sup>. The vast types of 2D materials display an extensive set of polaritons, including plasmons (interaction with free carriers), phonon polaritons (with optical phonons), exciton-polaritons (with excitons), magnon polaritons (with spin resonances), and Cooper-pair polaritons (with Cooper pairs). Due to the quantum confinement and the reduction of dielectric screening of the 2D layers, 2D polaritons exhibit the highest degree of confinement among all known materials, as well as several other excellent properties such as dynamical tunability<sup>[109]</sup>.

### **vdWHs**

2D materials consist of a single- or few-atom-thick, covalently-bonded lattices. Such dangling-bond-free atomic sheets often exhibit extraordinary electronic and optical properties, in contrast to nanostructures plagued with dangling bonds and trap states at the surface. In particular, 2D materials can be mechanically isolated, mixed, and matched, combining highly disparate atomic layers to create a wide range of vdWHs without the constraints of lattice matching and processing compatibility. This allows considerable freedom to create diverse vdWHs with functionalities that were not previously possible.

## Engineering polaritons in vdWHs

A variety of fabricated vdWHs have been shown to exhibit extraordinary performances and novel functionalities compared with pristine 2D materials. From the macro and micro perspectives, we divide the coupling and modulation mechanisms of different polaritons in vdWHs into the following types (as shown in Table 1). Macroscopic mechanisms: (1) dielectric engineering and (2) coupling to optical structures; Microscopic mechanisms: (1) Band-structure engineering and (2) coupling to other quasi-particles. Since plasmon and exciton polaritons are the results of resonance behavior sustained by charge carriers, an externally applied field can easily control the charge behavior, so understandably, several studies have exploited microscopic mechanisms to modulate such plasmon and exciton polaritons. In contrast, phonon polaritons are limited by the rigidity of lattice vibrations, so current research methods find it difficult to directly change the material crystal lattice, and therefore, their modulation has so far resorted on macroscopic mechanisms except the strain modulation.

### Box 2: General dispersion relationship of 2D polaritons in vdWHs

The dielectric function of 2D materials is generally divided into the following three categories, assuming a dielectric tensor of the form

$$\begin{Bmatrix} \varepsilon_x & 0 & 0 \\ 0 & \varepsilon_y & 0 \\ 0 & 0 & \varepsilon_z \end{Bmatrix},$$

which captures most situations of current interest:

- (1) Isotropic polaritonic materials:  $\varepsilon_x = \varepsilon_y = \varepsilon_z < 0$
- (2) Uniaxial hyperbolic polaritonic materials:  $\varepsilon_x = \varepsilon_y > 0, \varepsilon_z < 0$  or  $\varepsilon_x = \varepsilon_y < 0, \varepsilon_z > 0$
- (3) Biaxial anisotropic polaritonic materials:  $\varepsilon_x \neq \varepsilon_y \neq \varepsilon_z$  and  $\varepsilon_i < 0$  ( $i \in \{x, y, z\}$ )

Considering a vdWH of the form air/vdW1/vdW2, due to the extreme absorption of the polariton modes, the dispersion can be calculated from the poles of the imaginary part of the Fresnel reflection coefficient ( $\text{Im}\{r_p\}$ ) for p polarization in the vdWH. Using the reflection coefficients of the 1-2 (air/vdW1) and 2-3 (vdW1/vdW2) interfaces, which are given by

$$r_{12} = \frac{\varepsilon_{2z}k_1^z - \varepsilon_{1z}k_2^z}{\varepsilon_{2z}k_1^z + \varepsilon_{1z}k_2^z}$$

$$r_{23} = \frac{\varepsilon_{3z}k_2^z - \varepsilon_{2z}k_3^z}{\varepsilon_{3z}k_2^z + \varepsilon_{2z}k_3^z}$$

we obtain the reflection coefficient of the upper surface of the heterostructure as

$$r_p = \frac{r_{12} + r_{23}e^{i2k_2^z d}}{1 + r_{12}r_{23}e^{i2k_2^z d}}$$

where the subscripts 1, 2, and 3 correspond to air, vdW1, and vdW2 materials, respectively,  $d$  is the thickness of the vdW1 material, and  $k_j^z = \sqrt{\varepsilon_{ji}(\omega/c)^2 - (\varepsilon_{ji}/\varepsilon_z)q^2}$  with  $i \in \{x, y\}$  denotes the out-of-plane (along  $z$ ) light wave vector in medium  $j=1, 2, 3$ . A detailed analysis of the above expression yields the properties of polaritons in this type of structure, resulting from the dielectric permittivities of the constituents (i.e., the materials in the different layers). More complex structures can be studied following a similar type of analysis.

## Acknowledgements

This work was supported by the National Key R&D Program of China (2021YFA1201500), the National Natural Science Foundation of China (51925203, 52022025, 52102160, 51972074, 11674073, and U2032206), the Strategic Priority Research Program of the Chinese Academy of Sciences (XDB30000000 and XDB36000000), Youth Innovation Promotion Association CAS, C.A.S. Interdisciplinary Innovation Team (JCTD-2018-03), the

Open Project of Nanjing University (M34034), Academy of Finland (314810, 333982, 336144 and 336818), Academy of Finland Flagship Programme (320167, PREIN), the European Union's Horizon 2020 research and innovation program (820423, S2QUIP; 965124, FEMTOCHIP), the EU H2020-MSCA-RISE-872049 (IPN-Bio), the European Research Council (834742 and Advanced Grant 789104-eNANO), the Spanish MINECO (PID2020-112625GB-I00 and Severo Ochoa CEX2019-000910-S). X. Guo, and W. Lyu contributed equally to this work.

## Conflict of Interest

The authors declare no conflict of interest.

## References

- [1] a) W. Bogaerts, D. Pérez, J. Capmany, D. A. B. Miller, J. Poon, D. Englund, F. Morichetti, A. Melloni, *Nature* **2020**, 586, 207; b) U. Koch, C. Uhl, H. Hettrich, Y. Fedoryshyn, C. Hoessbacher, W. Heni, B. Baeuerle, B. I. Bitachon, A. Josten, M. Ayata, H. Xu, D. L. Elder, L. R. Dalton, E. Mentovich, P. Bakopoulos, S. Lischke, A. Krüger, L. Zimmermann, D. Tsiokos, N. Pleros, M. Möller, J. Leuthold, *Nat. Electron.* **2020**, 3, 338.
- [2] a) N. Rivera, I. Kaminer, *Nat. Rev. Phys.* **2020**, 2, 538; b) R. Chikkaraddy, B. de Nijs, F. Benz, S. J. Barrow, O. A. Scherman, E. Rosta, A. Demetriadou, P. Fox, O. Hess, J. J. Baumberg, *Nature* **2016**, 535, 127.
- [3] Y. Luo, R. Engelke, M. Mattheakis, M. Tamagnone, S. Carr, K. Watanabe, T. Taniguchi, E. Kaxiras, P. Kim, W. L. Wilson, *Nat. Commun.* **2020**, 11, 4209.
- [4] S. Dai, Q. Ma, M. K. Liu, T. Andersen, Z. Fei, M. D. Goldflam, M. Wagner, K. Watanabe, T. Taniguchi, M. Thiemens, F. Keilmann, G. C. A. M. Janssen, S. E. Zhu, P. Jarillo Herrero, M. M. Fogler, D. N. Basov, *Nat. Nanotechnol.* **2015**, 10, 682.

[5] X. Lin, Y. Yang, N. Rivera, J. J. López, Y. Shen, I. Kaminer, H. Chen, B. Zhang, J. D. Joannopoulos, M. Soljačić, *Proc. Natl. Acad. Sci.* **2017**, 114, 6717.

[6] a)D. N. Basov, M. M. Fogler, F. J. García de Abajo, *Science* **2016**, 354, aag1992; b)N. Li, X. Guo, X. Yang, R. Qi, T. Qiao, Y. Li, R. Shi, Y. Li, K. Liu, Z. Xu, L. Liu, F. J. García de Abajo, Q. Dai, E.-G. Wang, P. Gao, *Nat. Mater.* **2021**, 20, 43.

[7] a)G. X. Ni, A. S. McLeod, Z. Sun, L. Wang, L. Xiong, K. W. Post, S. S. Sunku, B. Y. Jiang, J. Hone, C. R. Dean, M. M. Fogler, D. N. Basov, *Nature* **2018**, 557, 530; b)H. Hu, R. Yu, H. Teng, D. Hu, N. Chen, Y. Qu, X. Yang, X. Chen, A. S. McLeod, P. Alonso-González, X. Guo, C. Li, Z. Yao, Z. Li, J. Chen, Z. Sun, M. Liu, F. J. García de Abajo, Q. Dai, *Nat. Commun.* **2022**, 13, 1465; c)Z. Zheng, J. Chen, Y. Wang, X. Wang, X. Chen, P. Liu, J. Xu, W. Xie, H. Chen, S. Deng, N. Xu, *Adv. Mater.* **2018**, 30, e1705318; d)W. Ma, P. Alonso-González, S. Li, A. Y. Nikitin, J. Yuan, J. Martín-Sánchez, J. Taboada-Gutiérrez, I. Amenabar, P. Li, S. Vélez, C. Tollar, Z. Dai, Y. Zhang, S. Sriram, K. Kalantar-Zadeh, S.-T. Lee, R. Hillenbrand, Q. Bao, *Nature* **2018**, 562, 557.

[8] a)C. Wu, X. Guo, Y. Duan, W. Lyu, H. Hu, D. Hu, K. Chen, Z. Sun, T. Gao, X. Yang, Q. Dai, *Adv. Mater.* **2022**, 34, 2110525; b)A. T. Costa, P. A. D. Gonçalves, D. N. Basov, F. H. L. Koppens, N. A. Mortensen, N. M. R. Peres, *Proc. Natl. Acad. Sci.* **2021**, 118, e2012847118; c)I. Epstein, D. Alcaraz, Z. Huang, V.-V. Pusapati, J.-P. Hugonin, A. Kumar, X. M. Deputy, T. Khodkov, T. G. Rappoport, J.-Y. Hong, N. M. R. Peres, J. Kong, D. R. Smith, F. H. L. Koppens, *Science* **2020**, 368, 1219; d)M. Gullans, D. E. Chang, F. H. L. Koppens, F. J. García de Abajo, M. D. Lukin, *Phys. Rev. Lett.* **2013**, 111, 247401; e)J. N. Chen, M. Badioli, P. Alonso-Gonzalez, S. Thongrattanasiri, F. Huth, J. Osmond, M. Spasenovic, A. Centeno, A. Pesquera, P. Godignon, A. Z. Elorza, N. Camara, F. J. G. de Abajo, R. Hillenbrand, F. H. L. Koppens, *Nature* **2012**, 487, 77; f)Z. Fei, A. S. Rodin, G. O. Andreev, W. Bao, A. S. McLeod, M. Wagner, L. M. Zhang, Z. Zhao, M. Thiemens, G. Dominguez, M. M. Fogler, A. H. C. Neto, C. N. Lau, F. Keilmann, D. N. Basov, *Nature* **2012**, 487, 82.

[9] A. J. Giles, S. Dai, I. Vurgaftman, T. Hoffman, S. Liu, L. Lindsay, C. T. Ellis, N. Assefa, I. Chatzakis, T. L. Reinecke, J. G. Tischler, M. M. Fogler, J. H. Edgar, D. N. Basov, J. D. Caldwell, *Nat. Mater.* **2018**, 17, 134.

[10] F. Hu, Y. Luan, M. E. Scott, J. Yan, D. G. Mandrus, X. Xu, Z. Fei, *Nat. Photon.* **2017**, 11, 356.

[11] Z. Fei, M. E. Scott, D. J. Gosztola, J. J. Foley, J. Yan, D. G. Mandrus, H. Wen, P. Zhou, D. W. Zhang, Y. Sun, J. R. Guest, S. K. Gray, W. Bao, G. P. Wiederrecht, X. Xu, *Phys. Rev. B* **2016**, 94, 081402.

[12] Z. Li, F. Sun, Z. Zheng, J. Chen, A. V. Davydov, S. Deng, H. Zhang, H. Chen, F. Liu, *Nano Lett.* **2021**, 21, 1822.

[13] M. E. Berkowitz, B. S. Y. Kim, G. Ni, A. S. McLeod, C. F. B. Lo, Z. Sun, G. Gu, K. Watanabe, T. Taniguchi, A. J. Millis, J. C. Hone, M. M. Fogler, R. D. Averitt, D. N. Basov, *Nano Lett.* **2021**, 21, 308.

[14] a)D. Rodrigo, O. Limaj, D. Janner, D. Etezadi, F. J. García de Abajo, V. Pruneri, H. Altug, *Science* **2015**, 349, 165; b)S.-H. Oh, H. Altug, X. Jin, T. Low, S. J. Koester, A. P. Ivanov, J. B. Edel, P. Avouris, M. S. Strano, *Nat. Commun.* **2021**, 12, 3824; c)X. Yang, Z. Sun, T. Low, H. Hu, X. Guo, F. J. G. d. Abajo, P. Avouris, Q. Dai, *Adv. Mater.* **2018**, 30, 1704896; d)H. Hu, X. Yang, X. Guo, K. Khaliji, S. R. Biswas, F. J. García de Abajo, T. Low, Z. Sun, Q. Dai, *Nat. Commun.* **2019**, 10, 1131; e)H. Hu, X. Yang, F. Zhai, D. Hu, R. Liu, K. Liu, Z. Sun, Q. Dai, *Nat. Commun.* **2016**, 7, 12334.

[15] Q. Guo, R. Yu, C. Li, S. Yuan, B. Deng, F. J. García de Abajo, F. Xia, *Nat. Mater.* **2018**, 17, 986.

[16] K. Ohtani, B. Meng, M. Franckié, L. Bosco, C. Ndebeka-Bandou, M. Beck, J. Faist, *Sci. Adv.* **2019**, 5, eaau1632.

[17] M. Klein, B. H. Badada, R. Binder, A. Alfrey, M. McKie, M. R. Koehler, D. G. Mandrus, T. Taniguchi, K. Watanabe, B. J. LeRoy, J. R. Schaibley, *Nat. Commun.* **2019**, 10, 3264.

[18] H. S. Lee, D. H. Luong, M. S. Kim, Y. Jin, H. Kim, S. Yun, Y. H. Lee, *Nat. Commun.* **2016**, 7, 13663.

[19] a)Y. Wu, Q. Ou, S. Dong, G. Hu, G. Si, Z. Dai, C.-W. Qiu, M. S. Fuhrer, S. Mokkapati, Q. Bao, *Adv. Mater.* **2021**, 33, 2008070; b)Y. Wu, Q. Ou, Y. Yin, Y. Li, W. Ma, W. Yu, G. Liu, X. Cui, X. Bao, J. Duan, G. Álvarez-Pérez, Z. Dai, B. Shabbir, N. Medhekar, X. Li, C.-M. Li, P. Alonso-González, Q. Bao, *Nat. Commun.* **2020**, 11, 2646; c)J. Taboada-Gutiérrez, G. Álvarez-Pérez, J. Duan, W. Ma, K. Crowley, I. Prieto, A. Bylinkin, M. Autore, H. Volkova, K. Kimura, T. Kimura, M. H. Berger, S. Li, Q. Bao, X. P. A. Gao, I. Errea, A. Y. Nikitin, R. Hillenbrand, J. Martín-Sánchez, P. Alonso-González, *Nat. Mater.* **2020**, 19, 964.

[20] T. Low, A. Chaves, J. D. Caldwell, A. Kumar, N. X. Fang, P. Avouris, T. F. Heinz, F. Guinea, L. Martin-Moreno, F. Koppens, *Nat. Mater.* **2017**, 16, 182.

[21] a)J. F. Sierra, J. Fabian, R. K. Kawakami, S. Roche, S. O. Valenzuela, *Nat. Nanotechnol.* **2021**, 16, 856; b)D. Jariwala, T. J. Marks, M. C. Hersam, *Nat. Mater.* **2017**, 16, 170.

[22] a)A. Woessner, M. B. Lundeberg, Y. Gao, A. Principi, P. Alonso-González, M. Carrega, K. Watanabe, T. Taniguchi, G. Vignale, M. Polini, J. Hone, R. Hillenbrand, F. H. L. Koppens, *Nat. Mater.* **2015**, 14, 421; b)X. Yang, F. Zhai, H. Hu, D. Hu, R. Liu, S. Zhang, M. Sun, Z. Sun, J. Chen, Q. Dai, *Adv. Mater.* **2016**, 28, 2931.

[23] X. Guo, R. Liu, D. Hu, H. Hu, Z. Wei, R. Wang, Y. Dai, Y. Cheng, K. Chen, K. Liu, G. Zhang, X. Zhu, Z. Sun, X. Yang, Q. Dai, *Adv. Mater.* **2020**, 32, 1907105.

[24] I. Alonso Calafell, L. A. Rozema, D. Alcaraz Iranzo, A. Trenti, P. K. Jenke, J. D. Cox, A. Kumar, H. Bieliaiev, S. Nanot, C. Peng, D. K. Efetov, J.-Y. Hong, J. Kong, D. R. Englund, F. J. García de Abajo, F. H. L. Koppens, P. Walther, *Nat. Nanotechnol.* **2021**, 16, 318.

[25] E. H. Hasdeo, J. C. W. Song, *Nano Lett.* **2017**, 17, 7252.

[26] S. S. Sunku, G. X. Ni, B. Y. Jiang, H. Yoo, A. Sternbach, A. S. McLeod, T. Stauber, L. Xiong, T. Taniguchi, K. Watanabe, P. Kim, M. M. Fogler, D. N. Basov, *Science* **2018**, 362, 1153.

[27] a)G. Hu, Q. Ou, G. Si, Y. Wu, J. Wu, Z. Dai, A. Krasnok, Y. Mazor, Q. Zhang, Q. Bao, C.-W. Qiu, A. Alù, *Nature* **2020**, 582, 209; b)M. Chen, X. Lin, T. H. Dinh, Z. Zheng, J. Shen, Q. Ma, H. Chen, P. Jarillo-Herrero, S. Dai, *Nat. Mater.* **2020**, 19, 1307; c)Z. Zheng, F. Sun, W. Huang, J. Jiang, R. Zhan, Y. Ke, H. Chen, S. Deng, *Nano Lett.* **2020**, 20, 5301; d)J. Duan, N. Capote-Robayna, J. Taboada-Gutiérrez, G. Álvarez-Pérez, I. Prieto, J. Martín-Sánchez, A. Y. Nikitin, P. Alonso-González, *Nano Lett.* **2020**, 20, 5323.

[28] K. S. Novoselov, A. Mishchenko, A. Carvalho, A. H. Castro Neto, *Science* **2016**, 353, aac9439.

[29] Y. Liu, Y. Huang, X. Duan, *Nature* **2019**, 567, 323.

[30] Y. Kurman, R. Dahan, H. Sheinfux Hanan, K. Wang, M. Yannai, Y. Adiv, O. Reinhardt, H. G. Tizei Luiz, Y. Woo Steffi, J. Li, H. Edgar James, M. Kociak, H. L. Koppens Frank, I. Kaminer, *Science* **2021**, 372, 1181.

[31] a)S. J. Ahn, P. Moon, T.-H. Kim, H.-W. Kim, H.-C. Shin, E. H. Kim, H. W. Cha, S.-J. Kahng, P. Kim, M. Koshino, Y.-W. Son, C.-W. Yang, J. R. Ahn, *Science* **2018**, 361, 782; b)S. Lisi, X. Lu, T. Benschop, T. A. de Jong, P. Stepanov, J. R. Duran, F. Margot, I. Cucchi, E. Cappelli, A. Hunter, A. Tamai, V. Kandyba, A. Giampietri, A. Barinov, J. Jobst, V. Stalman, M. Leeuwenhoek, K. Watanabe, T. Taniguchi, L. Rademaker, S. J. van der Molen, M. P. Allan, D. K. Efetov, F. Baumberger, *Nat. Phys.* **2021**, 17, 189; c)S. Forti, S. Link, A. Stöhr, Y. Niu, A. A. Zakharov, C. Coletti, U. Starke, *Nat. Commun.* **2020**, 11, 2236; d)H. Yang, A. Liang, C. Chen, C. Zhang, N. B. M. Schroeter, Y. Chen, *Nat. Rev. Mater.* **2018**, 3, 341; e)J. Katoch, S. Ulstrup, R. J. Koch, S. Moser, K. M. McCreary, S. Singh, J. Xu, B. T. Jonker, R. K. Kawakami, A. Bostwick, E. Rotenberg, C. Jozwiak, *Nat. Phys.* **2018**, 14, 355; f)P. V. Nguyen, N. C. Teutsch, N. P. Wilson, J. Kahn, X. Xia, A. J. Graham, V. Kandyba, A. Giampietri, A. Barinov, G. C. Constantinescu, N. Yeung, N. D. M. Hine, X. Xu, D. H. Cobden, N. R. Wilson, *Nature* **2019**, 572, 220; g)C. Gong, E. M. Kim, Y. Wang, G. Lee, X. Zhang, *Nat. Commun.* **2019**, 10, 2657.

[32] a)Y. Liu, N. O. Weiss, X. Duan, H.-C. Cheng, Y. Huang, X. Duan, *Nat. Rev. Mater.* **2016**, 1, 16042; b)S.-J. Liang, B. Cheng, X. Cui, F. Miao, *Adv. Mater.* **2020**, 32, 1903800.

[33] a)Y. Cao, V. Fatemi, A. Demir, S. Fang, S. L. Tomarken, J. Y. Luo, J. D. Sanchez-Yamagishi, K. Watanabe, T. Taniguchi, E. Kaxiras, R. C. Ashoori, P. Jarillo-Herrero, *Nature* **2018**, 556, 80; b)Y. Cao, V. Fatemi, S. Fang, K. Watanabe, T. Taniguchi, E. Kaxiras, P. Jarillo-Herrero, *Nature* **2018**, 556, 43.

[34] a)W. Chen, Z. Sun, Z. Wang, L. Gu, X. Xu, S. Wu, C. Gao, *Science* **2019**, 366, 983; b)D. Zhong, K. L. Seyler, X. Linpeng, N. P. Wilson, T. Taniguchi, K. Watanabe, M. A. McGuire, K.-M. C. Fu, D. Xiao, W. Yao, X. Xu, *Nat. Nanotechnol.* **2020**, 15, 187.

[35] Y. Zhou, J. Sung, E. Brutschea, I. Esterlis, Y. Wang, G. Scuri, R. J. Gelly, H. Heo, T. Taniguchi, K. Watanabe, G. Zaránd, M. D. Lukin, P. Kim, E. Demler, H. Park, *Nature* **2021**, 595, 48.

[36] a)Y. Wu, J. Duan, W. Ma, Q. Ou, P. Li, P. Alonso-González, J. D. Caldwell, Q. Bao, *Nat. Rev. Phys.* **2022**, <https://doi.org/10.1038/s42254-022-00472-0>; b)Q. Zhang, G. Hu, W. Ma, P. Li, A. Krasnok, R. Hillenbrand, A. Alù, C.-W. Qiu, *Nature* **2021**, 597, 187; c)H. Lin, Z. Zhang, H. Zhang, K.-T. Lin, X. Wen, Y. Liang, Y. Fu, A. K. T. Lau, T. Ma, C.-W. Qiu, B. Jia, *Chem. Rev.* **2022**, <https://doi.org/10.1021/acs.chemrev.2c00048>; d)C. Luo, X. Guo, H. Hu, D. Hu, C. Wu, X. Yang, Q. Dai, *Adv. Opt. Mater.* **2020**, 8, 1901416; e)Z. Dai, G. Hu, Q. Ou, L. Zhang, F. Xia, F. J. Garcia-Vidal, C.-W. Qiu, Q. Bao, *Chem. Rev.* **2020**, 120, 6197; f)W. Ma, B. Shabbir, Q. Ou, Y. Dong, H. Chen, P. Li, X. Zhang, Y. Lu, Q. Bao, *InfoMat* **2020**, 2, 777.

[37] a)S. Dai, J. Zhang, Q. Ma, S. Kittiwatanakul, A. McLeod, X. Chen, S. G. Corder, K. Watanabe, T. Taniguchi, J. Lu, Q. Dai, P. Jarillo-Herrero, M. Liu, D. N. Basov, *Adv. Mater.* **2019**, 31, 1900251; b)K. Chaudhary, M. Tamagnone, X. Yin, C. M. Spägele, S. L. Oscurato, J. Li, C. Persch, R. Li, N. A. Rubin, L. A. Jauregui, K. Watanabe, T. Taniguchi, P. Kim, M. Wuttig, J. H. Edgar, A. Ambrosio, F. Capasso, *Nat. Commun.* **2019**, 10, 4487; c)T. G. Folland, A. Fali, S. T. White, J. R. Matson, S. Liu, N. A. Aghamiri, J. H. Edgar, R. F. Haglund, Y. Abate, J. D. Caldwell, *Nat. Commun.* **2018**, 9, 4371; d)X. Song, Z. Liu, J. Scheuer, Y. Xiang, K. Aydin, *J. Phys. D: Appl. Phys.* **2019**, 52, 164002; e)S. Abedini Dereshgi, M. C. Larciprete, M. Centini, A. A. Murthy, K. Tang, J. Wu, V. P. Dravid, K. Aydin, *ACS Appl. Mater. Interfaces.* **2021**, 13, 48981.

[38] a)L. Xiong, C. Forsythe, M. Jung, A. S. McLeod, S. S. Sunku, Y. M. Shao, G. X. Ni, A. J. Sternbach, S. Liu, J. H. Edgar, E. J. Mele, M. M. Fogler, G. Shvets, C. R. Dean, D. N. Basov, *Nat. Commun.* **2019**, 10, 4780; b)L. Xiong, Y. Li, M. Jung, C. Forsythe, S. Zhang, A. S. McLeod, Y. Dong, S. Liu, F. L. Ruta, C. Li, K. Watanabe, T. Taniguchi, M. M. Fogler, J. H. Edgar, G. Shvets, C. R. Dean, D. N. Basov, *Sci. Adv.* **2021**, 7, eabe8087.

[39] a)Q. Zhang, Q. Ou, G. Hu, J. Liu, Z. Dai, M. S. Fuhrer, Q. Bao, C.-W. Qiu, *Nano Lett.* **2021**, 21, 3112; b)K. Chaudhary, M. Tamagnone, M. Rezaee, D. K. Bediako, A. Ambrosio, P. Kim, F. Capasso, *Sci. Adv.* **2019**, 5, eaau7171; c)N. A. Aghamiri, G. Hu, A. Fali, Z. Zhang, J. Li, S. Balendhran, S. Walia, S. Sriram, J. H. Edgar,

S. Ramanathan, A. Alù, Y. Abate, *Nat. Commun.* **2022**, 13, 4511; d)J. Duan, G. Álvarez-Pérez, K. V. Voronin, I. Prieto, J. Taboada-Gutiérrez, V. S. Volkov, J. Martín-Sánchez, A. Y. Nikitin, P. Alonso-González, *Sci. Adv.* **2021**, 7, eabf2690; e)A. Fali, S. T. White, T. G. Folland, M. He, N. A. Aghamiri, S. Liu, J. H. Edgar, J. D. Caldwell, R. F. Haglund, Y. Abate, *Nano Lett.* **2019**, 19, 7725; f)J. Duan, F. J. Alfaro-Mozaz, J. Taboada-Gutiérrez, I. Dolado, G. Álvarez-Pérez, E. Titova, A. Bylinkin, A. I. F. Tresguerres-Mata, J. Martín-Sánchez, S. Liu, J. H. Edgar, D. A. Bandurin, P. Jarillo-Herrero, R. Hillenbrand, A. Y. Nikitin, P. Alonso-González, *Adv. Mater.* **2022**, 34, 2104954.

[40] a)I. Epstein, A. J. Chaves, D. A. Rhodes, B. Frank, K. Watanabe, T. Taniguchi, H. Giessen, J. C. Hone, N. M. R. Peres, F. H. L. Koppens, *2D Mater.* **2020**, 7, 035031; b)Z. Sun, J. Gu, A. Ghazaryan, Z. Shotan, C. R. Considine, M. Dollar, B. Chakraborty, X. Liu, P. Ghaemi, S. Kéna-Cohen, V. M. Menon, *Nat. Photon.* **2017**, 11, 491.

[41] a)S. G. Menabde, I.-H. Lee, S. Lee, H. Ha, J. T. Heiden, D. Yoo, T.-T. Kim, T. Low, Y. H. Lee, S.-H. Oh, M. S. Jang, *Nat. Commun.* **2021**, 12, 938; b)P. A. D. Gonçalves, T. Christensen, N. M. R. Peres, A.-P. Jauho, I. Epstein, F. H. L. Koppens, M. Soljačić, N. A. Mortensen, *Nat. Commun.* **2021**, 12, 3271; c)I.-H. Lee, D. Yoo, P. Avouris, T. Low, S.-H. Oh, *Nat. Nanotechnol.* **2019**, 14, 313; d)P. Alonso-González, A. Y. Nikitin, Y. Gao, A. Woessner, M. B. Lundeberg, A. Principi, N. Forcellini, W. Yan, S. Vélez, A. J. Huber, K. Watanabe, T. Taniguchi, F. Casanova, L. E. Hueso, M. Polini, J. Hone, F. H. L. Koppens, R. Hillenbrand, *Nat. Nanotechnol.* **2017**, 12, 31; e)N. Zhang, W. Luo, L. Wang, J. Fan, W. Wu, M. Ren, X. Zhang, W. Cai, J. Xu, *Nat. Commun.* **2022**, 13, 983.

[42] H. Sumikura, T. Wang, P. Li, A.-K. U. Michel, A. Heßler, L. Jung, M. Lewin, M. Wuttig, D. N. Chigrin, T. Taubner, *Nano Lett.* **2019**, 19, 2549.

[43] a)X. Liu, J. Yi, S. Yang, E.-C. Lin, Y.-J. Zhang, P. Zhang, J.-F. Li, Y. Wang, Y.-H. Lee, Z.-Q. Tian, X. Zhang, *Nat. Mater.* **2021**, 20, 1210; b)A. Fieramosca, L. Polimeno, V. Ardizzone, L. De Marco, M. Pugliese, V. Maiorano, M. De Giorgi, L. Dominici, G. Gigli, D. Gerace, D. Ballarini, D. Sanvitto, *Sci. Adv.* **2019**, 5, eaav9967; c)N. Lundt, Ł. Dusanowski, E. Sedov, P. Stepanov, M. M. Glazov, S. Klembt, M. Klaas, J. Beierlein, Y. Qin, S. Tongay, M. Richard, A. V. Kavokin, S. Höfling, C. Schneider, *Nat. Nanotechnol.* **2019**, 14, 770; d)H. Zhang, B. Abhiraman, Q. Zhang, J. Miao, K. Jo, S. Roccasecca, M. W. Knight, A. R. Davoyan, D. Jariwala, *Nat. Commun.* **2020**, 11, 3552; e)S. Latini, U. De Giovannini, E. J. Sie, N. Gedik, H. Hübener, A. Rubio, *Phys. Rev. Lett.* **2021**, 126, 227401; f)L. Lackner, M. Dusel, O. A. Egorov, B. Han, H. Knopf, F. Eilenberger, S. Schröder, K. Watanabe, T. Taniguchi, S. Tongay, C. Anton-Solanas, S. Höfling, C. Schneider, *Nat. Commun.* **2021**, 12, 4933.

[44] a)L. Kim, S. Kim, P. K. Jha, V. W. Brar, H. A. Atwater, *Nat. Mater.* **2021**, 20, 805; b)H. Liu, T. E. Gage, P. Singh, A. Jaiswal, R. D. Schaller, J. Tang, S. T. Park, S. K. Gray, I. Arslan, *Nano Lett.* **2021**, 21, 5842.

[45] a)S. Castilla, I. Vangelidis, V.-V. Pusapati, J. Goldstein, M. Autore, T. Slipchenko, K. Rajendran, S. Kim, K. Watanabe, T. Taniguchi, L. Martín-Moreno, D. Englund, K.-J. Tielrooij, R. Hillenbrand, E. Lidorikis, F. H. L. Koppens, *Nat. Commun.* **2020**, 11, 4872; b)P. Pons-Valencia, F. J. Alfaro-Mozaz, M. M. Wiecha, V. Bielek, I. Dolado, S. Vélez, P. Li, P. Alonso-González, F. Casanova, L. E. Hueso, L. Martín-Moreno, R. Hillenbrand, A. Y. Nikitin, *Nat. Commun.* **2019**, 10, 3242.

[46] H. Hajian, I. D. Rukhlenko, G. W. Hanson, E. Ozbay, *J. Phys. D: Appl. Phys.* **2021**, 54, 455102.

[47] M. He, S. I. Halimi, T. G. Folland, S. S. Sunku, S. Liu, J. H. Edgar, D. N. Basov, S. M. Weiss, J. D. Caldwell, *Adv. Mater.* **2021**, 33, 2004305.

[48] F. Hu, Y. Luan, J. Speltz, D. Zhong, C. H. Liu, J. Yan, D. G. Mandrus, X. Xu, Z. Fei, *Phys. Rev. B* **2019**, 100, 121301.

[49] a)F. J. Alfaro-Mozaz, S. G. Rodrigo, P. Alonso-González, S. Vélez, I. Dolado, F. Casanova, L. E. Hueso, L. Martín-Moreno, R. Hillenbrand, A. Y. Nikitin, *Nat. Commun.* **2019**, 10, 42; b)J. Yang, Z. E. Krix, S. Kim, J. Tang, M. Mayyas, Y. Wang, K. Watanabe, T. Taniguchi, L. H. Li, A. R. Hamilton, I. Aharonovich, O. P. Sushkov, K. Kalantar-Zadeh, *Acs Nano* **2021**, 15, 9134.

[50] a)W. Liu, Z. Ji, Y. Wang, G. Modi, M. Hwang, B. Zheng, V. J. Sorger, A. Pan, R. Agarwal, *Science* **2020**, 370, 600; b)Y. Chen, S. Miao, T. Wang, D. Zhong, A. Saxena, C. Chow, J. Whitehead, D. Gerace, X. Xu, S.-F. Shi, A. Majumdar, *Nano Lett.* **2020**, 20, 5292.

[51] a)D. J. Rizzo, B. S. Jessen, Z. Sun, F. L. Ruta, J. Zhang, J.-Q. Yan, L. Xian, A. S. McLeod, M. E. Berkowitz, K. Watanabe, T. Taniguchi, S. E. Nagler, D. G. Mandrus, A. Rubio, M. M. Fogler, A. J. Millis, J. C. Hone, C. R. Dean, D. N. Basov, *Nano Lett.* **2020**, 20, 8438; b)F. Hu, M. Kim, Y. Zhang, Y. Luan, K. M. Ho, Y. Shi, C. Z. Wang, X. Wang, Z. Fei, *Nano Lett.* **2019**, 19, 6058; c)Y. Dong, L. Xiong, I. Y. Phinney, Z. Sun, R. Jing, A. S. McLeod, S. Zhang, S. Liu, F. L. Ruta, H. Gao, Z. Dong, R. Pan, J. H. Edgar, P. Jarillo-Herrero, L. S. Levitov, A. J. Millis, M. M. Fogler, D. A. Bandurin, D. N. Basov, *Nature* **2021**, 594, 513; d)W. Zhao, S. Zhao, H. Li, S. Wang, S. Wang, M. I. B. Utama, S. Kahn, Y. Jiang, X. Xiao, S. Yoo, K. Watanabe, T. Taniguchi, A. Zettl, F. Wang, *Nature* **2021**, 594, 517; e)S. S. Sunku, D. Halbertal, R. Engelke, H. Yoo, N. R. Finney, N. Curreli, G. Ni, C. Tan, A. S. McLeod, C. F. B. Lo, C. R. Dean, J. C. Hone, P. Kim, D. N. Basov, *Nano Lett.* **2021**, 21, 1688.

[52] a)H. A. Fernandez, F. Withers, S. Russo, W. L. Barnes, *Adv. Opt. Mater.* **2019**, 7, 1900484; b)M. Sidler, P. Back, O. Cotlet, A. Srivastava, T. Fink, M. Kroner, E. Demler, A. Imamoglu, *Nat. Phys.* **2017**, 13, 255; c)J. I. A. Li, T. Taniguchi, K. Watanabe, J. Hone, C. R. Dean, *Nat. Phys.* **2017**, 13, 751.

[53] a)M. Zhou, *Phys. Rev. B* **2021**, 104, 045419; b)N. C. H. Hesp, I. Torre, D. Barcons-Ruiz, H. Herzig Sheinfux, K. Watanabe, T. Taniguchi, R. Krishna Kumar, F. H. L. Koppens, *Nat. Commun.* **2021**, 12, 1640; c)S. Sunku, D. Halbertal, T. Stauber, S. Chen, A. S. McLeod, A. Rikhter, M. E. Berkowitz, C. F. B. Lo, D. E. Gonzalez-Acevedo, J. C. Hone, C. R. Dean, M. M. Fogler, D. N. Basov, *Nat. Commun.* **2021**, 12, 1641; d)G. X. Ni, H. Wang, J. S. Wu, Z. Fei, M. D. Goldflam, F. Keilmann, B. Özyilmaz, A. H. Castro Neto, X. M. Xie, M. M. Fogler, D. N. Basov, *Nat. Mater.* **2015**, 14, 1217; e)T. Huang, X. Tu, C. Shen, B. Zheng, J. Wang, H. Wang, K. Khaliji, S. H. Park, Z. Liu, T. Yang, Z. Zhang, L. Shao, X. Li, T. Low, Y. Shi, X. Wang, *Nature* **2022**, 605, 63; f)F. Hu, S. R. Das, Y. Luan, T. F. Chung, Y. P. Chen, Z. Fei, *Phys. Rev. Lett.* **2017**, 119, 247402.

[54] a)B. Lyu, H. Li, L. Jiang, W. Shan, C. Hu, A. Deng, Z. Ying, L. Wang, Y. Zhang, H. A. Bechtel, M. C. Martin, T. Taniguchi, K. Watanabe, W. Luo, F. Wang, Z. Shi, *Nano Lett.* **2019**, 19, 1982; b)G. X. Ni, H. Wang, B. Y. Jiang, L. X. Chen, Y. Du, Z. Y. Sun, M. D. Goldflam, A. J. Frenzel, X. M. Xie, M. M. Fogler, D. N. Basov, *Nat. Commun.* **2019**, 10, 4360.

[55] L. Zhang, F. Wu, S. Hou, Z. Zhang, Y.-H. Chou, K. Watanabe, T. Taniguchi, S. R. Forrest, H. Deng, *Nature* **2021**, 591, 61.

[56] F. J. Bezares, A. D. Sanctis, J. R. M. Saavedra, A. Woessner, P. Alonso-González, I. Amenabar, J. Chen, T. H. Bointon, S. Dai, M. M. Fogler, D. N. Basov, R. Hillenbrand, M. F. Craciun, F. J. García de Abajo, S. Russo, F. H. L. Koppens, *Nano Lett.* **2017**, 17, 5908.

[57] a)A. Bylinkin, M. Schnell, M. Autore, F. Calavalle, P. Li, J. Taboada-Gutiérrez, S. Liu, J. H. Edgar, F. Casanova, L. E. Hueso, P. Alonso-Gonzalez, A. Y. Nikitin, R. Hillenbrand, *Nat. Photon.* **2021**, 15, 197; b)M. Autore, P. Li, I. Dolado, F. J. Alfaro-Mozaz, R. Esteban, A. Atxabal, F. Casanova, L. E. Hueso, P. Alonso-González, J. Aizpurua, A. Y. Nikitin, S. Vélez, R. Hillenbrand, *Light Sci. Appl.* **2018**, 7, 17172.

[58] a)M. Nalabothula, P. K. Jha, T. Low, A. Kumar, *Phys. Rev. B* **2020**, 102, 045416; b)M. K. Svendsen, Y. Kurman, P. Schmidt, F. Koppens, I. Kaminer, K. S. Thygesen, *Nat. Commun.* **2021**, 12, 2778.

[59] a)D. B. Farmer, D. Rodrigo, T. Low, P. Avouris, *Nano Lett.* **2015**, 15, 2582; b)D. Alcaraz Iranzo, S. Nanot, E. J. C. Dias, I. Epstein, C. Peng, D. K. Efetov, M. B. Lundeberg, R. Parret, J. Osmond, J.-Y. Hong, J. Kong, D. R. Englund, N. M. R. Peres, F. H. L. Koppens, *Science* **2018**, 360, 291; c)J. Nong, W. Wei, W. Wang, G. Lan, Z. Shang, J. Yi, L. Tang, *Opt. Express* **2018**, 26, 1633.

[60] a)F. C. B. Maia, B. T. O'Callahan, A. R. Cadore, I. D. Barcelos, L. C. Campos, K. Watanabe, T. Taniguchi, C. Deneke, A. Belyanin, M. B. Raschke, R. O. Freitas, *Nano Lett.* **2019**, 19, 708; b)X. G. Xu, J.-H. Jiang, L. Gilburd, R. G. Rensing, K. S. Burch, C. Zhi, Y. Bando, D. Golberg, G. C. Walker, *Acs Nano* **2014**, 8, 11305; c)F. L. Ruta, B. S. Y. Kim, Z. Sun, D. J. Rizzo, A. S. McLeod, A. Rajendran, S. Liu, A. J. Millis, J. C. Hone, D. N. Basov, *Nat. Commun.* **2022**, 13, 3719.

[61] I.-H. Lee, M. He, X. Zhang, Y. Luo, S. Liu, J. H. Edgar, K. Wang, P. Avouris, T. Low, J. D. Caldwell, S.-H. Oh, *Nat. Commun.* **2020**, 11, 3649.

[62] G. X. Ni, L. Wang, M. D. Goldflam, M. Wagner, Z. Fei, A. S. McLeod, M. K. Liu, F. Keilmann, B. Özyilmaz, A. H. Castro Neto, J. Hone, M. M. Fogler, D. N. Basov, *Nat. Photon.* **2016**, 10, 244.

[63] A. Woessner, Y. Gao, I. Torre, M. B. Lundeberg, C. Tan, K. Watanabe, T. Taniguchi, R. Hillenbrand, J. Hone, M. Polini, F. H. L. Koppens, *Nat. Photon.* **2017**, 11, 421.

[64] a)H. Hu, X. Guo, D. Hu, Z. Sun, X. Yang, Q. Dai, *Adv. Sci.* **2018**, 5, 1800175; b)I. D. Barcelos, A. R. Cadore, A. B. Alencar, F. C. B. Maia, E. Mania, R. F. Oliveira, C. C. B. Bufon, Á. Malachias, R. O. Freitas, R. L. Moreira, H. Chacham, *Acs Photon.* **2018**, 5, 1912.

[65] a)H. Li, M. I. B. Utama, S. Wang, W. Zhao, S. Zhao, X. Xiao, Y. Jiang, L. Jiang, T. Taniguchi, K. Watanabe, A. Weber-Bargioni, A. Zettl, F. Wang, *Nano Lett.* **2020**, 20, 3106; b)N. C. H. Hesp, M. K. Svendsen, K. Watanabe, T. Taniguchi, K. S. Thygesen, I. Torre, F. H. L. Koppens, *Nano Lett.* **2022**, 22, 6200.

[66] M. Yankowitz, Q. Ma, P. Jarillo-Herrero, B. J. LeRoy, *Nat. Rev. Phys.* **2019**, 1, 112.

[67] a)L. Jiang, Z. Shi, B. Zeng, S. Wang, J.-H. Kang, T. Joshi, C. Jin, L. Ju, J. Kim, T. Lyu, Y.-R. Shen, M. Crommie, H.-J. Gao, F. Wang, *Nat. Mater.* **2016**, 15, 840; b)B.-Y. Jiang, G.-X. Ni, Z. Addison, J. K. Shi, X. Liu, S. Y. F. Zhao, P. Kim, E. J. Mele, D. N. Basov, M. M. Fogler, *Nano Lett.* **2017**, 17, 7080.

[68] L. Brey, T. Stauber, T. Slipchenko, L. Martín-Moreno, *Phys. Rev. Lett.* **2020**, 125, 256804.

[69] M. B. Lundeberg, Y. Gao, R. Asgari, C. Tan, B. Van Duppen, M. Autore, P. Alonso-González, A. Woessner, K. Watanabe, T. Taniguchi, R. Hillenbrand, J. Hone, M. Polini, F. H. L. Koppens, *Science* **2017**, 357, 187.

[70] P. Alonso-González, A. Y. Nikitin, F. Golmar, A. Centeno, A. Pesquera, S. Vélez, J. Chen, G. Navickaite, F. Koppens, A. Zurutuza, F. Casanova, L. E. Hueso, R. Hillenbrand, *Science* **2014**, 344, 1369.

[71] M. Jung, Z. Fan, G. Shvets, *Phys. Rev. Lett.* **2018**, 121, 086807.

[72] a)P. Li, I. Dolado, F. J. Alfaro-Mozaz, F. Casanova, L. E. Hueso, S. Liu, J. H. Edgar, A. Y. Nikitin, S. Vélez, R. Hillenbrand, *Science* **2018**, 359, 892; b)Z. Zheng, N. Xu, S. L. Oscurato, M. Tamagnone, F. Sun, Y. Jiang, Y. Ke, J. Chen, W. Huang, W. L. Wilson, A. Ambrosio, S. Deng, H. Chen, *Sci. Adv.* **2019**, 5, eaav8690; c)G. Hu, J. Shen, C.-W. Qiu, A. Alù, S. Dai, *Adv. Opt. Mater.* **2020**, 8, 1901393.

[73] a)A. Ambrosio, M. Tamagnone, K. Chaudhary, L. A. Jauregui, P. Kim, W. L. Wilson, F. Capasso, *Light Sci. Appl.* **2018**, 7, 27; b)J. Duan, R. Chen, J. Li, K. Jin, Z. Sun, J. Chen, *Adv. Mater.* **2017**, 29, 1702494.

[74] a)G. Álvarez-Pérez, A. González-Morán, N. Capote-Robayna, K. V. Voronin, J. Duan, V. S. Volkov, P. Alonso-González, A. Y. Nikitin, *Ac Photon.* **2022**, 9, 383; b)S. Dai, Z. Fei, Q. Ma, A. S. Rodin, M. Wagner, A. S. McLeod, M. K. Liu, W. Gannett, W. Regan, K. Watanabe, T. Taniguchi, M. Thiemens, G. Dominguez, A. H. C. Neto, A. Zettl, F. Keilmann, P. Jarillo-Herrero, M. M. Fogler, D. N. Basov, *Science* **2014**, 343, 1125.

[75] a)P. Li, X. Yang, T. W. W. Masz, J. Hanss, M. Lewin, A.-K. U. Michel, M. Wuttig, T. Taubner, *Nat. Mater.* **2016**, 15, 870; b)M. Wuttig, H. Bhaskaran, T. Taubner, *Nat. Photon.* **2017**, 11, 465; c)C. Zheng, R. E. Simpson, K. Tang, Y. Ke, A. Nemati, Q. Zhang, G. Hu, C. Lee, J. Teng, J. K. W. Yang, J. Wu, C.-W. Qiu, *Chem. Rev.* **2022**; d)Z. Shao, X. Cao, H. Luo, P. Jin, *Npg Asia Mater.* **2018**, 10, 581.

[76] A. M. Dubrovkin, B. Qiang, H. N. S. Krishnamoorthy, N. I. Zheludev, Q. J. Wang, *Nat. Commun.* **2018**, 9, 1762.

[77] a)S. Dai, Q. Ma, T. Andersen, A. S. McLeod, Z. Fei, M. K. Liu, M. Wagner, K. Watanabe, T. Taniguchi, M. Thiemens, F. Keilmann, P. Jarillo-Herrero, M. M. Fogler, D. N. Basov, *Nat. Commun.* **2015**, 6, 6963 ; b)P. Li, M. Lewin, A. V. Kretinin, J. D. Caldwell, K. S. Novoselov, T. Taniguchi, K. Watanabe, F. Gaussmann, T. Taubner, *Nat. Commun.* **2015**, 6, 7507.

[78] X. Liu, T. Galfsky, Z. Sun, F. Xia, E.-c. Lin, Y.-H. Lee, S. Kéna-Cohen, V. M. Menon, *Nat. Photon.* **2015**, 9, 30.

[79] J. Wen, H. Wang, W. Wang, Z. Deng, C. Zhuang, Y. Zhang, F. Liu, J. She, J. Chen, H. Chen, S. Deng, N. Xu, *Nano Lett.* **2017**, 17, 4689.

[80] S. Dhara, C. Chakraborty, K. M. Goodfellow, L. Qiu, T. A. O'Loughlin, G. W. Wicks, S. Bhattacharjee, A. N. Vamivakas, *Nat. Phys.* **2018**, 14, 130.

[81] J. Gu, V. Walther, L. Waldecker, D. Rhodes, A. Raja, J. C. Hone, T. F. Heinz, S. Kéna-Cohen, T. Pohl, V. M. Menon, *Nat. Commun.* **2021**, 12, 2269.

[82] a)N. Lundt, S. Klembt, E. Cherotchenko, S. Betzold, O. Iff, A. V. Nalitov, M. Klaas, C. P. Dietrich, A. V. Kavokin, S. Höfling, C. Schneider, *Nat. Commun.* **2016**, 7, 13328; b)C. Schneider, M. M. Glazov, T. Korn, S. Höfling, B. Urbaszek, *Nat. Commun.* **2018**, 9, 2695.

[83] C. Anton-Solanas, M. Waldherr, M. Klaas, H. Suchomel, T. H. Harder, H. Cai, E. Sedov, S. Klembt, A. V. Kavokin, S. Tongay, K. Watanabe, T. Taniguchi, S. Höfling, C. Schneider, *Nat. Mater.* **2021**, 20, 1233.

[84] a)R. P. A. Emmanuele, M. Sich, O. Kyriienko, V. Shahnazaryan, F. Withers, A. Catanzaro, P. M. Walker, F. A. Benimetskiy, M. S. Skolnick, A. I. Tartakovskii, I. A. Shelykh, D. N. Krizhanovskii, *Nat. Commun.* **2020**, 11, 3589; b)R. Verre, D. G. Baranov, B. Munkhbat, J. Cuadra, M. Käll, T. Shegai, *Nat. Nanotechnol.* **2019**, 14, 679.

[85] X. Zhang, C. De-Eknakul, J. Gu, A. L. Boehmke, V. M. Menon, J. Khurgin, E. Cubukcu, *Nat. Nanotechnol.* **2019**, 14, 844.

[86] Z. Wang, D. A. Rhodes, K. Watanabe, T. Taniguchi, J. C. Hone, J. Shan, K. F. Mak, *Nature* **2019**, 574, 76.

[87] J. Christensen, A. Manjavacas, S. Thongrattanasiri, F. H. L. Koppens, F. J. García de Abajo, *Ac Nano* **2012**, 6, 431.

[88] S. Wang, S. Yoo, S. Zhao, W. Zhao, S. Kahn, D. Cui, F. Wu, L. Jiang, M. I. B. Utama, H. Li, S. Li, A. Zibrov, E. Regan, D. Wang, Z. Zhang, K. Watanabe, T. Taniguchi, C. Zhou, F. Wang, *Nat. Commun.* **2021**, 12, 5039.

[89] G. Hu, A. Krasnok, Y. Mazor, C.-W. Qiu, A. Alù, *Nano Lett.* **2020**, 20, 3217.

[90] V. W. Brar, M. S. Jang, M. Sherrott, S. Kim, J. J. Lopez, L. B. Kim, M. Choi, H. Atwater, *Nano Lett.* **2014**, 14, 3876.

[91] a)Y. Jia, H. Zhao, Q. Guo, X. Wang, H. Wang, F. Xia, *Ac Photon.* **2015**, 2, 907; b)A. Kumar, T. Low, K. H. Fung, P. Avouris, N. X. Fang, *Nano Lett.* **2015**, 15, 3172.

[92] F. Ghohroodi Ghamsari, R. Asgari, *Plasmonics* **2020**, 15, 1289.

[93] Y. Jiang, X. Lin, T. Low, B. Zhang, H. Chen, *Laser Photonics Rev.* **2018**, 12, 1800049.

[94] J.-W. Kang, B. Song, W. Liu, S.-J. Park, R. Agarwal, C.-H. Cho, *Sci. Adv.* **2019**, 5, eaau9338.

[95] W. Du, T. Wang, H.-S. Chu, C. A. Nijhuis, *Nat. Photon.* **2017**, 11, 623.

[96] Y. Wang, J. Yu, Y.-F. Mao, J. Chen, S. Wang, H.-Z. Chen, Y. Zhang, S.-Y. Wang, X. Chen, T. Li, L. Zhou, R.-M. Ma, S. Zhu, W. Cai, J. Zhu, *Nature* **2020**, 581, 401.

[97] I. Alonso Calafell, J. D. Cox, M. Radonjić, J. R. M. Saavedra, F. J. García de Abajo, L. A. Rozema, P. Walther, *Npj Quantum Inf.* **2019**, 5, 37.

[98] W. Lyu, H. Teng, C. Wu, X. Zhang, X. Guo, X. Yang, Q. Dai, *Nanoscale* **2021**, 13, 12720.

[99] S. Yuan, D. Naveh, K. Watanabe, T. Taniguchi, F. Xia, *Nat. Photon.* **2021**, 15, 601.

[100] M. D. Fraser, S. Höfling, Y. Yamamoto, *Nat. Mater.* **2016**, 15, 1049.

[101] a)X. Guo, N. Li, C. Wu, X. Dai, R. Qi, T. Qiao, T. Su, D. Lei, N. Liu, J. Du, E. Wang, X. Yang, P. Gao, Q. Dai, *Adv. Mater.* **2022**, 2201120; b)C. Song, X. Yuan, C. Huang, S. Huang, Q. Xing, C. Wang, C. Zhang, Y. Xie, Y. Lei, F. Wang, L. Mu, J. Zhang, F. Xiu, H. Yan, *Nat. Commun.* **2021**, 12, 386.

[102] S. Guddala, F. Komissarenko, S. Kiriushechkina, A. Vakulenko, M. Li, V. M. Menon, A. Alù, A. B. Khanikaev, *Science* **2021**, 374, 225.

[103] J. Duan, G. Álvarez-Pérez, A. I. F. Tresguerres-Mata, J. Taboada-Gutiérrez, K. V. Voronin, A. Bylinkin, B. Chang, S. Xiao, S. Liu, J. H. Edgar, J. I. Martín, V. S. Volkov, R. Hillenbrand, J. Martín-Sánchez, A. Y. Nikitin, P. Alonso-González, *Nat. Commun.* **2021**, 12, 4325.

[104] Q. Zhang, Q. Ou, G. Si, G. Hu, S. Dong, Y. Chen, J. Ni, C. Zhao, M. S. Fuhrer, Y. Yang, A. Alù, R. Hillenbrand, C.-W. Qiu, *Sci. Adv.* **2018**, 8, eabn9774.

[105] D. J. Rizzo, S. Shabani, B. S. Jessen, J. Zhang, A. S. McLeod, C. Rubio-Verdú, F. L. Ruta, M. Cothrine, J. Yan, D. G. Mandrus, S. E. Nagler, A. Rubio, J. C. Hone, C. R. Dean, A. N. Pasupathy, D. N. Basov, *Nano Lett.* **2022**, 22, 1946.

[106] A. V. Zasedatelev, A. V. Baranikov, D. Sannikov, D. Urbonas, F. Scafirimuto, V. Y. Shishkov, E. S. Andrianov, Y. E. Lozovik, U. Scherf, T. Stöferle, R. F. Mahrt, P. G. Lagoudakis, *Nature* **2021**, 597, 493.

[107] Z. Yang, T. Albrow-Owen, W. Cai, T. Hasan, *Science* **2021**, 371, eabe0722.

[108] R. Yu, A. Manjavacas, F. J. García de Abajo, *Nat. Commun.* **2017**, 8, 2.

[109] F. J. García de Abajo, *Acsl Photon.* **2014**, 1, 135.

# Accepted Article



Xiangdong Guo is a Postdoc in Qing Dai's group at the National Center of Nanoscience and Technology, China. He received his bachelor's degree in applied physics from Fuzhou University in 2015 and Ph.D. degree in condensed matter physics from Peking University in 2020. His present research mainly focuses on nanophotonics and polaritonics based on 2D materials.



Wei Lyu is a master's student jointly trained by Qing Dai's group at the National Center for Nanoscience and Technology and Tianjin University. He is currently completing a Ph.D. in the College of Engineering and Applied Sciences at Nanjing University. His present research focuses on 2D materials and optoelectronics.



Xiaoxia Yang is a Professor of Nanophotonics in Qing Dai's group at the National Center for Nanoscience and Technology, China. She received her Ph.D. degree in condensed matter physics from Institute of Physics, Chinese Academy of Sciences in 2012. Her research interests currently focus on low-dimensional materials and nanophotonics.



Qing Dai is a Professor at the National Center for Nanoscience and Technology, China. He received his M.Eng. in electronic and electrical engineering from Imperial College, London, in 2007 and Ph.D. in nanophotonics from the Department of Engineering, University of Cambridge in 2011. His main research interests are low-dimensional materials, optoelectronics, and nanophotonics.

**ToC text:** We review the state of the art of 2D material polaritons in van der Waals heterostructures (vdWHs) from the perspective of design principles and potential applications. We start by discussing some fundamental properties of polaritons in vdWHs, and then cover recent discoveries of plasmons, phonon polaritons, exciton polaritons and their hybrid modes in vdWHs, respectively.

## ToC figure

# Accepted Article

